Chemical Science

ROYAL SOCIETY OF CHEMISTRY

REVIEW

View Article Online
View Journal

Cite this: DOI: 10.1039/d5sc10169g

Photocrosslinking chemistry for direct photopatterning of colloidal nanocrystals: toward pixelated light emitting diodes and beyond

Wenyue Qing and Hao Zhang *

Colloidal quantum dots (QDs) exhibit outstanding optoelectronic properties and solution processability, making them promising candidates for devices such as quantum dot light emitting diodes (QLEDs). The realization of integrated QD-based devices, particularly in QLED displays, necessitates patterning techniques that offer high resolution, high fidelity, and preserved luminescence. Direct photopatterning *via* photocrosslinking chemistry has emerged as a promising strategy, which achieves microscale to nanoscale patterning by using light-triggered reactions of surface ligands to modulate QD colloidal stability without compromising their optical properties. This review outlines recent advances in photocrosslinking-enabled direct photopatterning of QDs for QLED applications. We begin by introducing the underlying mechanisms and representative photochemistries for direct patterning. Subsequently, we survey various photocrosslinking chemistries and their applications in QD patterning. Drawing on case studies of representative photocrosslinking mechanisms, we discuss key molecular design principles for crosslinkers toward high-performance QLEDs. Furthermore, we extend the discussion to patterning of other functional nanomaterials, such as metal–organic frameworks, and to three-dimensional QD printing. Finally, we conclude with an outlook on future developments and the broadening applications of photocrosslinking-enabled patterning technologies.

Received 29th December 2025
Accepted 30th March 2026

DOI: 10.1039/d5sc10169g

rsc.li/chemical-science

1 Introduction

QDs are promising nanomaterials for next-generation electronic and photonic devices, owing to their outstanding optoelectronic properties and solution processability.[1–7] For instance, combined attributes of wide colour gamut, narrow spectral bandwidths, and near-unity photoluminescent quantum yield (PLQY) of QDs enables the rapid developments of QLEDs and commercialization of QD televisions, among others.[8–20] However, the integration of QDs, or more generally functional nanocrystals (NCs), into system-level devices requires precise deposition of QD patterns with micro- or even nanoscale precision, which necessitates high-resolution and high-fidelity patterning techniques.[20,21] Over the past few

Department of Chemistry, Center for BioAnalytical Chemistry, Key Laboratory of Bioorganic Phosphorus Chemistry & Chemical Biology (Ministry of Education), Tsinghua University, Beijing 100084, China. E-mail: hzhangchem@mail.tsinghua.edu.cn

Wenyue Qing

Wenyue Qing is a PhD candidate in Prof. Hao Zhang's group at Tsinghua University. She completed her undergraduate study at Sichuan University in 2022. Her research is focused on direct photopatterning of QDs and their integration into optoelectronic devices.

Hao Zhang

Hao Zhang is now an associate professor in Department of Chemistry, Tsinghua University. He obtained his PhD in Department of Chemistry at University of Chicago in 2015 and conducted postdoctoral research at Northwestern University from 2016 to 2018. He joined his current position in 2019. His current research is focused on the surface chemistry enabled patterning and printing of functional nanomaterials and optoelectronic devices.

decades, various QD patterning methods have been developed, including inkjet printing, transfer printing, and lithography.[17,20,22–29]

Conventional lithography typically involves complex, multi-step processes and the use of photoresists whose solvents and chemicals could degrade the optoelectronic properties of QDs, presenting a significant bottleneck for device performance.[28,29] Inkjet printing technology could achieve large-area, high-throughput, and low-cost patterning, but it is limited by nozzle size and the coffee-ring effect, typically restricting its resolution to tens to hundreds of micrometers.[22,23] Transfer printing technology, by constructing micro- and nano-scale stamps, has demonstrated significant potential in achieving sub-micron-level high resolution. Recent research advances in this field have been quite encouraging, showcasing improved techniques and material compatibility.[24–26] However, it is generally acknowledged that scaling these promising developments for large-scale industrial production remains a considerable challenge. In this context, the emergence of direct optical lithography of functional inorganic nanomaterials (DOLFIN), proposed by Talapin group in 2017, offers a ground breaking photoresist-free strategy for QD patterning and their integrated device applications.[31] The core mechanism of this approach is altering the QD dispersibility through surface photochemical reactions of ligands *via* UV light stimulus. Compared to traditional lithography, DOLFIN, or more generally direct photopatterning process, is greatly simplified by consisting of only film deposition, UV exposure, and developing steps. This straightforward procedure, along with the elimination of harsh irradiation, unfavourable chemicals, and other detrimental processes, has established direct photopatterning as a highly promising method for QD patterning. Over the past years, a variety of photochemical mechanisms and designs for direct photopatterning have been developed by researchers across the world, utilizing ligand decomposition, desorption, crosslinking, and stripping mechanisms.[31–67] These advancements have led to direct photopatterning techniques that preserve the optoelectronic properties of QDs and enabled the fabrication of high-performance QLED arrays.

Among these photochemistries, the ligand crosslinking approach is particularly noteworthy for making patterned QDs with high photoluminescent (PL) and electroluminescent (EL) performance.[32–40] First, these ligand crosslinking chemistries involve QDs with well-passivated surface by their original or photocrosslinkable ligands, representing a nondestructive approach to preserve the luminescent properties of the QDs. Second, many groups including us have developed various ligand crosslinking methods for direct photopatterning of QDs and relevant pixelated devices. These studies include the use of crosslinkable ligands, dual ligands, and additive, nonspecific or specific crosslinkers. Data from these studies and rich chemical designs are critical for providing an in-depth summary of representative advances and key design principles of the photochemistries for direct photopatterning of QDs. Last but not least, rationally designed photocrosslinking chemistries have enabled full-colour, high-resolution (over 15 875 ppi),[34] and precise patterning of luminescent QDs and NCs (II–VI, III–V, and lead halide based perovskites) with fully preserved PLQYs.[33,34,36–38] The EL characteristics of patterned QLEDs made with these chemistries have also reached the stage of being comparable with their nonpatterned counterparts, with encouraging demos in passive- or active-matrix-driven QLED displays.[34,36,38]

In this review, we highlight the remarkable progress made during the past five years in photocrosslinking-enabled direct photopatterning of QDs and their applications in QLEDs. Recently, several representative reviews and perspectives have been dedicated to summarizing these developments and elaborating on the relationship between patterning chemistry and device performance.[41–48] Distinguished from previous work, this review offers a focused analysis in three key aspects: (1) a focused photocrosslinking pathway analysis. While covering representative types of direct photopatterning chemistries, we place particular emphasis on photocrosslinking pathways, which have demonstrated strong compatibility with passive- and active-matrix backplanes and enabled the fabrication of high-performance pixelated QLEDs. (2) From mechanism to patterned QLEDs. We systematically summarize design principles for photocrosslinkers toward highly luminescent QD patterns, review recent progress in directly photopatterned QLED performance, and provide guidelines for further development of patterning chemistries. (3) Extended applications and outlook. Beyond conventional 2D patterning, we also discuss the emerging role of photochemistry in 3D printing and offer perspectives on next-generation photocrosslinkers with functionalities that extend beyond patterning. In this review, we start by briefly introducing the mechanisms of photopatterning and representative types of photochemistries involved. Second, we provide a comprehensive survey of different types of photocrosslinking chemistries and their applications in QD patterning. Third, we propose key molecular design principles for photocrosslinkers toward high-performance QLEDs based on the data from studies on representative crosslinkers. Fourth, we extend the discussion to more recent advances on the crosslinking-based patterning of other functional nanomaterials (*e.g.* MOFs) and QD printing in three dimensions. Finally, we conclude with an outlook on future developments and the expanding applications of photocrosslinking-enabled patterning technique.

2 Fundamentals of direct photopatterning of colloidal NCs

2.1 Comparison of traditional and resist-free direct photolithography of NCs

Direct photopatterning relies on the interplay of surface photochemistry and colloidal stability of QDs. Photochemical reactions taken place on QD surface upon light or other stimuli change the QD dispersibility. The irradiation-induced solubility changes, as with traditional photolithography, set the basis of direct photopatterning. However, direct photopatterning does not involve photoresists, leading to much fewer steps than traditional photolithography, as shown in Scheme 1. Direct

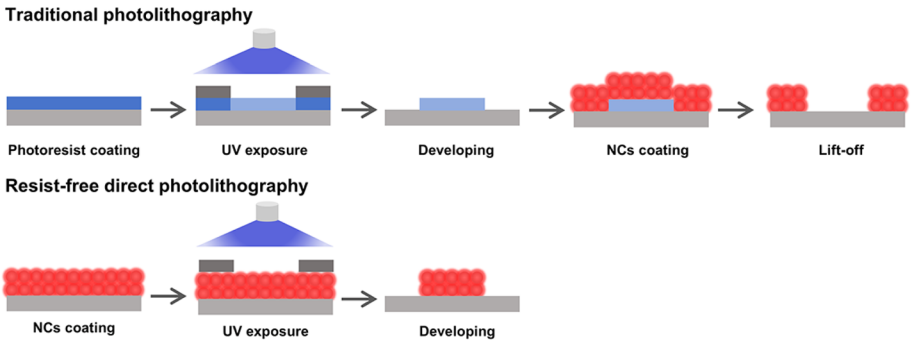

Scheme 1 Comparison of patterning steps between traditional and resist-free direct photolithography. Both cases show the negative-tone patterning.

photolithography effectively preserves the intrinsic physicochemical and luminescent properties of patterned QDs by fundamentally avoiding the detrimental chemical exposures inherent in conventional photolithography—such as those from photoresists, developers, and etching agents.[30]

2.2 Various photochemistries for NC patterning

The advancement of direct photopatterning for NCs is fundamentally rooted in the exploitation of specific photochemical reactions that modulate colloidal stability. These methods can be broadly categorized into four representative mechanistic classes (Scheme 2): ligand decomposition, ligand desorption, ligand crosslinking, and ligand binding, each employing a distinct pathway to cause solubility contrast of NCs between exposed and unexposed regions.

2.2.1 Ligand decomposition. The strategy of ligand decomposition relies on the photolytic cleavage of specially designed, photosensitive ligands that are anchored to the NC surface. Upon light exposure, the decomposition of these ligands alters the surface chemistry, leading to a reduction in interparticle repulsive forces and subsequent colloidal destabilization. A seminal example is the work by the Talapin group, which introduced 1,2,3,4-thiatriazole-5-thiolate (TTT) as a photo-decomposable ligand.[31] Under 254 nm UV irradiation, TTT ligands on the QD surface decompose into SCN^-, N_2, and sulfur. The generated SCN^-, compared to the TTT ligands, provided poorer electrostatic repulsion, leading to QDs with much lower solubility. Therefore, QD films in the UV-exposed regions remained insoluble during solvent development, forming well-defined QD patterns. Subsequently, Wang *et al.* expanded the toolbox of photo-decomposable ligands to include dithiocarbamates, azoles, xanthates, and thiooxalates, thereby extending the operational spectral range from deep UV (254 nm) to the visible region (450 nm).[49] These decomposable ligands provide a negative-tone patterning mechanism where the irradiated regions become insoluble, and its effectiveness is directly related to the reaction rate of the photodecomposition of ligands.

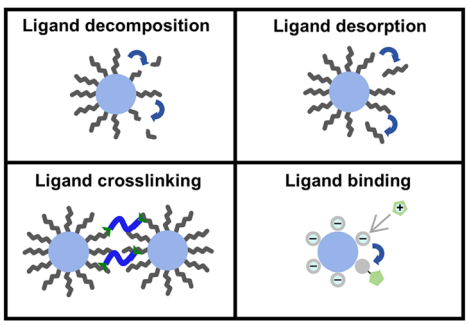

Scheme 2 Four representative photochemistries for direct patterning, including ligand decomposition, ligand desorption, ligand crosslinking, and ligand binding.

2.2.2 Ligand desorption. The mechanism of ligand desorption centers on the light-triggered removal of stabilizing ligands from the NC surface, thereby decreasing the ligand density and diminishing the steric or electrostatic repulsion that maintains colloidal stability. A prominent method involves the use of photoacid generators (PAGs). For instance, 2-(4-methoxystyryl)-4,6-bis(trichloromethyl)-1,3,5-triazine (MBT), upon UV exposure, releases strong acids (*e.g.*, HCl) which protonate the native Lewis basic ligands (*e.g.*, oleic acid), prompting their desorption from NC surface.[31,50] NCs with reduced ligand coverage in the exposed regions then remain in patterned layers after solvent development. Beside PAGs, certain ligands themselves are designed to detach upon irradiation. Methacrylate-based ligands, for example, can detach from the QD surface under UV light exposure.[51] The ligand desorption pathway effectively transforms a stable colloidal dispersion into an unstable one in the exposed zones, enabling high-fidelity patterning. Its versatility allows it to be applied to a broad class of NCs stabilized by weakly coordinating organic ligands. Moreover, our group employed triphenylchloromethane (TPCl) as a photosensitive stripping agent. Upon irradiation, the Lewis acidic triphenyl carbocation generated from TPCl photolysis can effectively strip the native ligands from QD surfaces *via* a Lewis acid–base reaction, thereby reducing the solubility of QDs in nonpolar solvents. Meanwhile, the chloride ions produced from TPCl photolysis can passivate the uncoordinated surface sites, thus effectively preserving the optoelectronic properties of the QDs.[39]

2.2.3 Ligand crosslinking. Crosslinkable ligands or crosslinker additives connect surface aliphatic ligands on

neighbouring QDs upon light exposure and create insoluble network of crosslinked QDs in the exposed region. QDs with native ligands can be crosslinked upon high-energy irradiation source such as e-beam or X-ray. However, this approach often suffers from limited scalability and can degrade the optoelectronic properties of QDs due to radiation damage.[52–54] Recent studies have thus focused on developing milder, UV light-driven crosslinking schemes.[32–40,55–64] This is achieved by incorporating crosslinkable functional groups into the surface ligands or adding small molecular crosslinkers. Examples of such photocrosslinkable moieties include azides, diazirines, acrylates, thiols, and benzophenones, all of which can efficiently bridge native aliphatic ligands under benign conditions. As mentioned in the Introduction, this strategy can preserve the degree of surface passivation and is particularly advantageous for creating patterned QD layers and devices with excellent luminescent properties.

2.2.4 Ligand binding. The ligand binding mechanism is mostly applicable to electrostatically stabilized QDs. This process introduces photogenerated strongly coordinating species, which bind to the QD surface and neutralize the charges, thereby screening electrostatic repulsion and reducing colloidal stability. For example, diazonaphthosulfonic acid (DNS),[58] when introduced to bare QDs stabilized with positive surface charges, can photodecompose to produce carboxylic acid derivatives that possess a high affinity to the QD surface. This photo-induced ligand binding process effectively neutralizes the positively charged surface, leading to QD destabilization. Similarly, PAGs are employed in this context releasing a high concentration of photogenerated protons that directly neutralize negatively charged NC surfaces.[31] This ion-binding mechanism offers a direct and efficient route for patterning QDs stabilized by ionic forces, complementing the strategies designed for sterically stabilized systems.

3 Photocrosslinking chemistries for direct photopatterning of NCs

Photocrosslinking-enabled direct patterning has emerged as an effective strategy to achieve nondestructive, high-definition, and high-throughput NC patterns. The core mechanism is to form covalent bonds between the ligands of neighbouring QDs upon photochemical reactions of crosslinkable ligands or additive crosslinkers. Here, three categories of representative photocrosslinking chemistries will be discussed and compared, including crosslinkable ligands, dual ligands, and additive crosslinkers.

3.1 Rationale of photocrosslinking chemistry as an adaptive strategy

Ligand surface passivation is a critical determinant for both the high PLQY and the stability of QDs, serving as a key factor for their optoelectronic performance in device applications. Several patterning methods involve ligand exchange or ligand removal, processes that inevitably introduce surface defect states and trap sites, leading to pronounced PLQY degradation through nonradiative recombination. In contrast, photocrosslinking-enabled patterning, typically implemented *via* additive crosslinkers or photosensitive long-chain ligands, maintains high surface ligand coverage and effective passivation. More specifically, additive-crosslinker-based approach can retain the native ligands, which are already optimized for effective surface passivation during synthesis, thereby preserving the high luminescent properties of the as-prepared QDs.

Beyond optical performance, photocrosslinking also offers distinct practical advantages for scalable manufacturing: (1) process compatibility and ease of operation. When using additive crosslinkers, the method requires no ligand exchange—only the direct addition of crosslinker to the original QD solution. This seamlessly integrates with existing commercial QD inks and established QLED fabrication processes. (2) Material stability and scalability. In crosslinking approaches, QDs remain protected either by their original organic ligands or by designed long-chain photocrosslinkable ligands, ensuring excellent colloidal stability and extended shelf lifetime—key attributes for reproducible large-scale production. (3) Solvent versatility and environmental adaptability. Through rational design of dispersing ligands or photocrosslinkable ligands, QDs can be dispersed in solvents spanning a wide polarity range, including environmentally friendly options.[34,61] This tuneable solubility enhances compatibility with industrial printing and coating processes, further supporting the transition toward scalable manufacturing.

3.2 Different classes of photocrosslinking chemistry

3.2.1 Crosslinkable ligands. Early studies revealed that high-energy stimuli (*e.g.*, electron beams) can cleave C–H or C=C bonds in native ligands (*e.g.*, oleylamine or oleic acid) on QDs, thereby promoting the formation of new C=C or C–C bonds between adjacent ligands and ultimately leading to QD crosslinking.[52–54] However, the reliance on high-energy sources limits its application in large-scale, low-cost patterning, and the irradiation can severely quench the luminescence of QDs. In comparison, photochemically initiated ligand crosslinking operates under much gentler exposure conditions and demonstrates superior compatibility with standard photolithographic methods. Bang and co-workers developed a random semiconducting polymer ligand, PTPA-N_3-SH, which integrates a triphenylamine-based hole-transporting moiety with a UV-crosslinkable azide group (Fig. 1a).[59] The patterning capability of the method enables the fabrication of features as small as 5 μm. QLED devices based on the resulting patterned QDs achieved a maximum external quantum efficiency (EQE_{max}) of 6% and a maximum luminance (L_{max}) exceeding 11 000 cd m^{-2}, demonstrating both high resolution and promising electroluminescent performance. They further designed a poly(2-cinnamoyloxyethyl) methacrylate crosslinkable ligand which enables perovskite NC patterning by utilizing [2 + 2] cycloaddition reaction between adjacent olefin groups upon 365 nm UV irradiation.[60] This photocyclization mechanism directly connects individual NCs into a crosslinked network structure. This dual-functional ligand enables direct photopatterning of

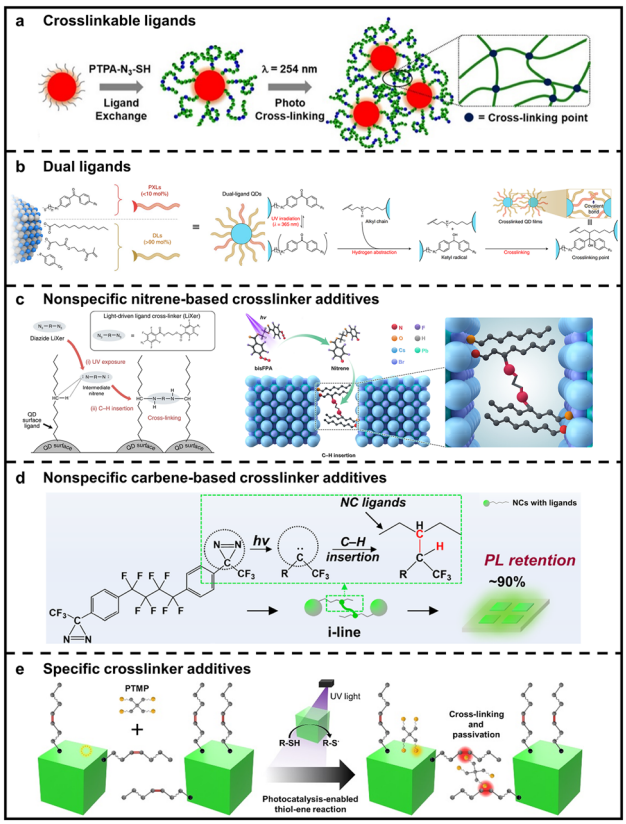

Fig. 1 Representative photocrosslinking chemistries for QD direct photopatterning. (a) Crosslinkable ligands.[59] Adapted with permission from ref. 59. Copyright 2020 American Chemical Society. (b) Dual ligands, including crosslinking ligands and dispersing ligands.[34] Adapted with permission from ref. 34. Copyright 2022 Springer Nature. (c) Nonspecific nitrene-based crosslinker additives.[35,55] Adapted with permission from ref. 35 and 55. Copyright 2022 American Association for the Advancement of Science and 2020 Springer Nature. (d) Nonspecific carbene-based crosslinker additives.[37] Adapted with permission from ref. 37. Copyright 2024 American Chemical Society. (e) Specific thiol-based crosslinker additives.[56] Adapted with permission from ref. 56. Copyright 2023 American Association for the Advancement of Science.

lead halide-based perovskite NC films under UV light irradiation, achieving microscale feature sizes (<10 μm) while fully preserving their high luminescence.

3.2.2 Dual ligands. Hahm *et al.* developed a new crosslinking-enabled patterning method that employs QDs passivated with dual ligands (Fig. 1b).[34] In this approach, a dual-ligand system is employed, comprising a small fraction (<10 mol%) of photocrosslinkable ligands (PXLs) and a predominant proportion (>90 mol%) of dispersing ligands (DLs). Under UV irradiation, the PXLs undergo covalent crosslinking, enabling high-resolution photopatterning while preserving the optical properties of the QDs. Concurrently, the DLs maintain colloidal stability and tailor solvent compatibility, ensuring the QD inks are adaptable to various solution-processing techniques. Specifically, in Hahm's system, the PXLs are benzophenone derivatives functionalized at the *para* position with groups such as pyrrolidinyl (–N(CH_2)$_4$), oxy (–O–), or thio (–S–) to fine-tune their photochemical reactivity. The DLs include oleic acid (OA), mono-2-(methacryloyloxy) ethyl succinate (MMES), or 4-(trifluoromethyl) benzenethiolate (TFMBT), each providing tailored colloidal stability and solvent adaptability that enables processing in media ranging from polar organic solvents like propylene glycol methyl ether acetate (PGMEA) and diethylene glycol monoethyl ether acetate (DGMEA) to fluorinated solvents such as trifluorotoluene. Upon 365 nm irradiation, the benzophenone derivatives generate reactive carbonyl radicals that drive C–H insertion into the aliphatic chains of neighbouring ligands, forming a crosslinked network. This strategy enables the fabrication of full-colour, high-resolution QD patterns (>15 000 ppi) under mild UV doses and with minimal photocrosslinker content, seamlessly integrating into industrial-standard microfabrication processes. The patterned QDs exhibit virtually no loss in intrinsic optical properties, while the fabricated QLEDs achieve high device performance, with EQE approaching 20% for red-emitting CdSe QLED devices. The approach further demonstrates excellent compatibility with scalable, large-area processing techniques, as exemplified by the uniform patterning of multicolour QDs across six-inch silicon wafers, underscoring its effectiveness for advanced photonic and display applications.

Lately, Lee *et al.* introduces a bifunctional ligand/crosslinker, 4-(3-trifluoromethyl)-3*H*-diazirin-3-yl) benzoic acid (TDBA), which integrates both a carboxylate anchoring group and a photoactive diazirine moiety.[63] By enabling a surface-anchored, direct crosslinking mechanism, this strategy not only circumvents the optical deterioration associated with ligand exchange but also significantly enhances crosslinking density and pattern fidelity. Moreover, Wang group recently developed a class of photosensitive ligands incorporating methacrylate and carboxyl groups that enable direct photopatterning of QDs in industrial compatible solvents such as PGMEA.[61] Through ligand exchange, these dual-functional molecules anchor onto QD surfaces *via* their carboxyl groups, conferring colloidal stability in PGMEA while rendering the QDs photosensitive. Upon exposure to 365 or 405 nm light, the methacrylate units undergo crosslinking, enabling high-resolution patterning without the need for additional photopolymerizable additives.

Replacing the original ligands on the QD surface with functional new ligands requires repeated solvent/anti-solvent washing steps and exposes the QDs to air, likely leading to a decline in colloidal stability and a reduction in luminescent performance. Thus Kwak *et al.* designed a bifunctional FPA-S ligand that integrates both photo-induced ligand exchange and photo-crosslinking capabilities.[64] With a dihydrolipoic acid (DHLA) moiety at one end for robust anchoring onto QD surfaces *via* photoligation, and an azide group at the other end for photocrosslinking, this ligand enables rapid and stable *in situ* ligand exchange for InP-based QDs, realizing high-resolution QD patterning and enhanced performance in QLEDs.

3.2.3 Crosslinker additives. The aforementioned two photocrosslinking approaches are limited by their reliance on ligand exchange for QDs, which requires careful control to prevent degradation of their optoelectronic properties.

Furthermore, they may suffer from inherent batch-to-batch variations in ligand-exchange extent and resulting ligand ratios on QD surface, making it difficult to achieve reproducible and uniform device performance in large-scale manufacturing. To circumvent issues associated with ligand exchange—including the introduction of surface defects and inconsistent ligand replacement—researchers have developed strategies involving the introduction of photosensitive crosslinkers. In this mechanism, crosslinker additives bearing at least two reactive sites are incorporated into the system to bridge the native long-chain ligands of adjacent QDs. Based on whether the crosslinking reaction requires the QD ligands to possess particular functional groups beyond nonspecific saturated bonds such as C–H or C–C, photocrosslinkers can be classified into specific and nonspecific types.

Nonspecific crosslinkers offer broad compatibility with native ligand shells, enabling patterning across diverse QD compositions without requiring surface pre-modification. Certain nonspecific crosslinking strategies—such as those based on benzophenone or carbene chemistry—have been shown to be nondestructive, preserving QD luminescence without compromising efficiency. However, this generality often comes at the cost of lower reaction selectivity, which can lead to side reactions and potential quenching of QD luminescence, as noted in Section 4.1.4. In contrast, specific crosslinkers (*e.g.*, thiol-ene click chemistry) provide high reaction selectivity and efficiency, which minimizes side reactions and byproducts. Nevertheless, their application usually necessitates QD surfaces to be pre-functionalized with complementary reactive groups, adding complexity to material synthesis and processing.

Common nonspecific crosslinker additives include nitrene- and carbene-based crosslinkers. Kang group reported a nitrene-based crosslinker, ethane-1,2-diyl bis(4-azido-2,3,5,6-tetrafluorobenzoate) (abbreviated as EBT), to achieve crosslinking QD patterns (Fig. 1c, left).[55] EBT crosslinkers generate reactive nitrene intermediates upon 254 nm irradiation, which then undergo nonspecific C–H insertion reactions with the native long-chain ligands (such as oleylamines and oleic acids), thereby connecting adjacent QDs. This crosslinking mechanism enables photopatterning at ultralow exposure doses of only 2–3 mJ cm^{-2} while reaching a fine resolution of 2 μm. Importantly, the patterned QDs retain their original PLQY, and red-emitting devices fabricated with the crosslinked CdSe/CdZnS QD layers exhibit EQE as high as 14.6%, matching the performance of devices prepared from pristine QDs.

EBT crosslinkers can also enable direct photopatterning of perovskite NCs. Liu *et al.* developed a method named DOPPLCER, which achieved high-resolution patterning of perovskite NCs down to 5 μm (Fig. 1c, right).[35] Upon exposure to 254 nm light at 60 mJ cm^{-2}, the patterned perovskite NC film retained 63% of its original PLQY. Importantly, a post-treatment step further enhanced the relative PLQY retention to approximately 125%. When incorporated into light-emitting devices, the crosslinked $FAPbBr_3$ perovskite LEDs realized a record EQE of 6.8% and luminance over 2×10^4 cd m^{-2}, establishing new performance benchmarks for patterned perovskite LEDs at the time.

In parallel, our group developed a photosensitive carbene-based crosslinker 3,3′-(4,4′-(perfluorobutane-1,4-diyl) bis(4,1-phenylene)) bis(3-(trifluoromethyl)-3*H*-diazirine, which effectively undergo C–H insertion with neighbouring long-chain ligands under 365 nm exposure in nitrogen atmosphere (Fig. 1d).[37] Compared to nitrene-based crosslinker, this carbene-based crosslinker is much milder and thus suitable for more fragile NCs such as perovskites. Thus this approach based on carbene-based crosslinker could retain 90% PLQY of pristine $CsPbBr_3$ films. Crosslinked $FAPbBr_3$ LEDs achieved a L_{max} exceeding 60 000 cd m^{-2} and an EQE_{max} of 16%. This represents a significant improvement of PL and EL performance over the DOPPLCER method using nitrene-based crosslinkers.

Specific crosslinkers react exclusively with particular functional groups (*e.g.*, C=C bonds) of surface ligands on QDs. A common strategy employs thiol-terminated crosslinkers that, under UV light, undergo a thiol–ene reaction with C=C groups of the native ligands to form C–S covalent bonds. Cho group employed pentaerythritol tetrakis(3-mercaptopropionate) as a dual-role crosslinker, whose four terminal thiol groups generate radicals upon UV irradiation (Fig. 1e).[56] These thiol radicals rapidly undergo photo-induced thiol-ene click reactions with the C=C bonds of native ligands on the perovskite NC surface, forming stable C–S linkages. By leveraging the inherent photocatalytic activity of the perovskite material itself, this system significantly enhances the reaction efficiency and lowers the required exposure dose to only ≈30 mJ cm^{-2} under 275 nm irradiation. Consequently, high-resolution multicolour patterning (<1 μm) is achieved with complete preservation of the luminescent properties. Moreover, the crosslinkers concurrently serve as a surface-passivating agent, further improving the PLQY and photo-stability of the patterned perovskite NCs. These thiol additives are also demonstrated to be applied to nondestructive patterning of InP QDs as well.[62]

More recently, Lee group systematically compared dithiol crosslinkers TBBT and BPDT for patterning Cd-based QDs.[65] Although both maintained high PLQY, BPDT-based devices achieved higher EQE (9.73% *vs.* 6.83%). DFT calculations revealed that BPDT's biphenyl structure enhances π-orbital overlap and charge injection, providing molecular-level insights for crosslinker design. Maeng *et al.* screened dithiol crosslinkers for perovskite NC patterning, finding that longer carbon chains (C8–C12) reduced the required concentrations of crosslinkers by two orders of magnitude.[66] 1,8-Octanedithiol and 1,10-decanedithiol emerged as optimal due to their solvent compatibility and stability. Combined with post-patterning exchanges, efficient perovskite NC LEDs were fabricated. The $CsPbBr_3$ patterned devices reached a EQE_{max} of 14.7% and luminescence over 25 400 cd m^{-2}, while $CsPbBr_xI_{3-x}$ patterned devices achieved a EQE_{max} of 13.1% and L_{max} of 637 cd m^{-2}.

3.2.4 Metrics for evaluating patterning quality. The performance of devices based on patterned QD films is profoundly influenced by the quality of the patterned films. A representative set of key metrics for evaluating patterning efficacy consists of resolution, which dictates both image clarity and device integration density; scalability, which determines the throughput and industrial compatibility; and pattern

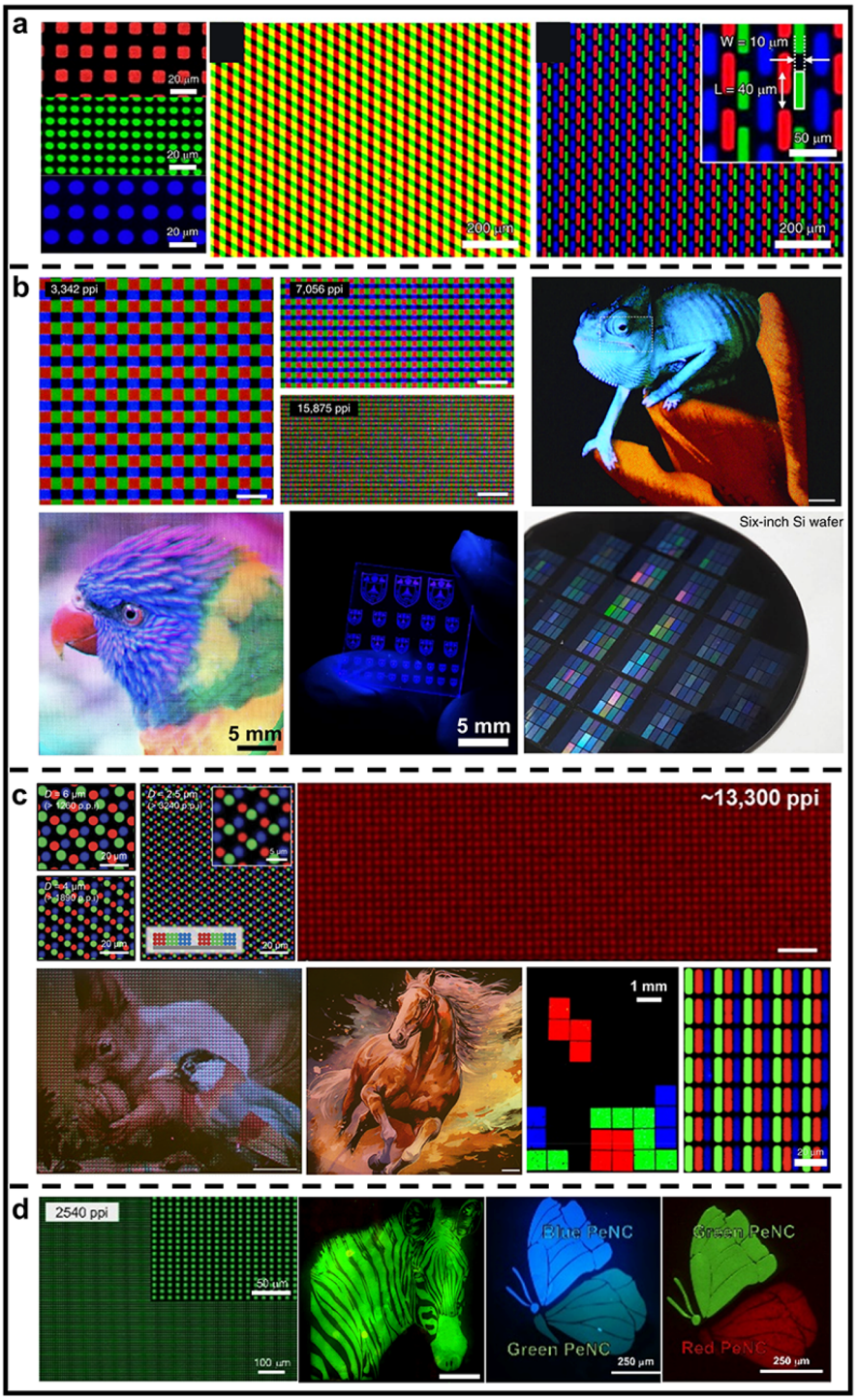

Fig. 2 Representative patterns achieved *via* different photocrosslinking mechanisms, showing the patterning resolution, scalability, and fidelity. (a) Patterned *via* crosslinkable ligands containing azide or cinnamoyl groups.[59,60] Adapted with permission from ref. 59 and 60. Copyright 2020 American Chemical Society and 2021 American Chemical Society. (b) Patterned *via* dual ligands, with crosslinking ligands containing benzophenone or methacrylate groups.[34,38] Adapted with permission from ref. 34 and 38. Copyright 2022 Springer Nature and 2025 Springer Nature. (c) Patterned *via* nonspecific nitrene- or carbene-based crosslinkers.[33,36,37,55,57] Adapted with permission from ref. 33, 36, 37, 55 and 57. Copyright 2022 Wiley-VCH, 2024 American Chemical Society, 2024 American Chemical Society, 2020 Springer Nature, and 2024 Springer Nature. (d) Patterned *via* specific thiol-based crosslinkers.[56] Adapted with permission from ref. 56. Copyright 2023 American Association for the Advancement of Science.

quality, which governs the fidelity. These criteria collectively form a foundational standard for assessing and comparing different patterning methods. Fig. 2 shows QD patterns formed *via* different photocrosslinking approaches, namely crosslinkable ligands (Fig. 2a), dual ligands (Fig. 2b), nonspecific crosslinker (Fig. 2c), and specific crosslinkers (Fig. 2d).

4 Design principles for photocrosslinkers toward high-performance pixelated QLEDs

The pursuit of high-performance patterned QLEDs requires photolithographic strategies that are effective in patterning while nondestructive toward the intrinsic optoelectronic properties of QDs. A central challenge is that the introduced photosensitive crosslinkers could trigger nonradiative recombination pathways at the QD surface and induce undesirable side reactions, compromising luminescent efficiency and charge transport properties. This section focuses on key chemical design principles for photocrosslinkers that minimize damage to QDs, preserve or even enhance QD properties, and enable the fabrication of high-performance, patterned QLEDs (Scheme 3). In the following, we take the widely studied nitrene- and carbene-based crosslinkers as examples to explain each of the design principles in detail and illustrate how chemical design addresses associated challenges and requirements with case studies.

4.1 Design principles for photocrosslinkers

4.1.1 Spectral response. The spectral response of the photochemical process is a critical consideration in direct optical patterning of QDs, as deep UV exposure—typically required to trigger the crosslinking reaction—can induce severe photodamage to the QD surface. This includes photo-oxidation, the formation of dangling bonds and the creation of trap states, all of which significantly degrade luminescent properties of QDs.[68,69] This highlights the importance of rationally modulating the spectral response of photocrosslinkers, as patterning with longer-wavelength, lower-energy light significantly reduces the risk of photodamage to QDs (Scheme 3a and b). Based on previous experiments, the use of nitrene-based crosslinkers such as EBT requires exposure to deep UV irradiation at 254 nm, which significantly reduces the PLQY retention of crosslinked QD films.[32] Here, we will discuss three strategies for red-shifting the spectral response of photocrosslinkers and reducing photodamages.

4.1.1.1 Conjugated group functionalization. In our earlier work, structural functionalization was attempted on nitrene-based crosslinkers by introducing conjugated groups to red-shift their absorption wavelength (Fig. 3a).[32] Although this approach successfully shifted the absorption maximum from 254 nm to 365 nm, it concurrently lowered the electronic energy levels of the crosslinkers, which facilitated electron transfer from the QDs, thereby inducing luminescence quenching.

4.1.1.2 Photocrosslinkers with extended absorption. Beyond functionalizing deep UV-sensitive crosslinkers towards longer-wavelength absorption, an alternative approach involves exploring other classes of photocrosslinkers. For instance, our group developed carbene-based crosslinkers for nondestructive QD patterning and systematically investigated their photochemical process and impacts on QD properties (Fig. 3a and b).[32] Upon light irradiation, carbene-based crosslinkers generate reactive carbene intermediates, which undergo nonspecific C–H insertion with the native ligands of QDs to achieve crosslinked patterns. Compared to nitrene-based crosslinkers, carbene-based crosslinkers possess longer-wavelength spectral response. The extended absorption spectrum of carbene-based crosslinkers (200−400 nm) enables QD patterning at longer wavelengths (*e.g.*, 365 nm, i-line), thereby reducing UV-induced photodamage to QDs. This also aligns with optoelectronic characterization results. Carbene-based patterning of Cd-based QD films achieves ≈90% PLQY

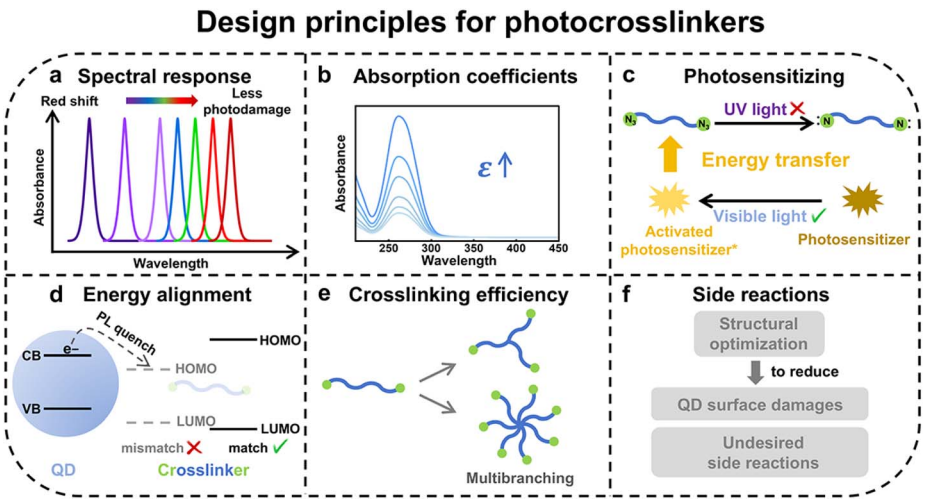

Scheme 3 Design principles for photocrosslinkers. Key chemical design principles for photocrosslinkers includes spectral response of longer wavelengths, energy alignment between photocrosslinkers and QDs, faster main reaction rate, and minimized side reactions.

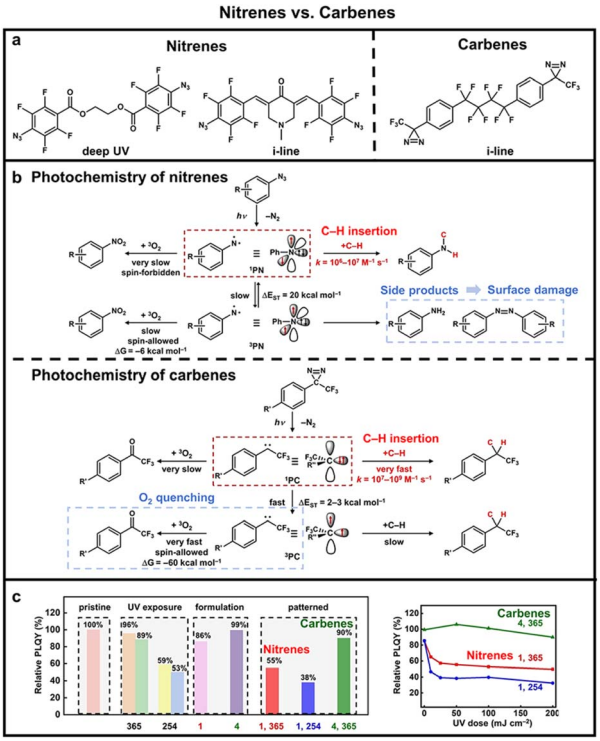

Fig. 3 Comparison of nitrene- and carbene-based crosslinkers. (a) Molecular structures of nitrene- and carbene-based crosslinkers designed for spectral shifting.[32] (b) Different photochemitries of nitrene- and carbene-based crosslinkers.[32] (c) Efficacy of nitrene- and carbene-based crosslinkers in maintaining the PL properties of QDs.[32] Adapted with permission from ref. 32. Copyright 2022 Wiley-VCH.

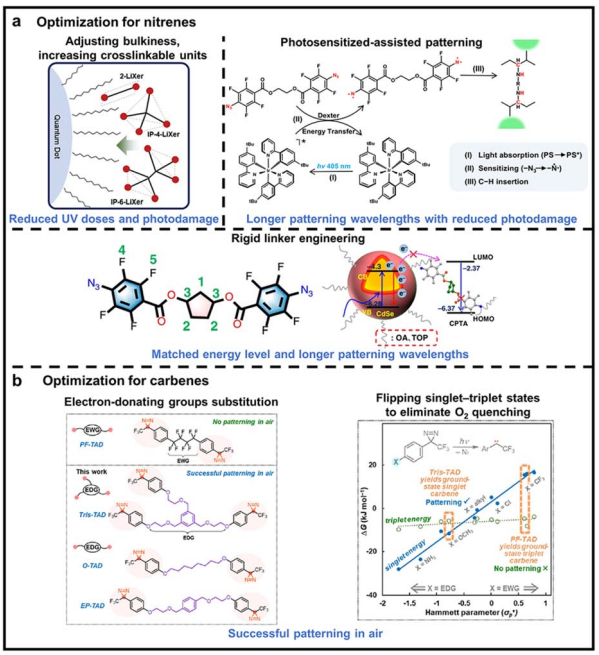

Fig. 4 Optimization of nitrene- and carbene-based crosslinkers to address the proposed design principles. (a and b) Optimization for (a) nitrene- and (b) carbene-based crosslinkers for minimizing damages to QDs.[33,36,57,70] Adapted with permission from ref. 33, 36, 57 and 70. Copyright 2022 Wiley-VCH, 2024 American Chemical Society, 2024 Springer Nature, and 2025 Springer Nature.

retention, whereas azide-based patterning only retains ≈55% PLQY (Fig. 3c).

4.1.1.3 Photosensitizing. We proposed another photosensitizer-assisted approach for direct QD photopatterning, which employs $Ir(tBu\text{-}ppy)_3$ to absorb h-line (405 nm) light and activate nitrene-based crosslinkers *via* Dexter energy transfer, generating nitrene intermediates for ligand crosslinking (Scheme 3c and Fig. 4a, right).[57] This approach successfully red-shifted the required wavelength of nitrene-based crosslinkers from deep ultraviolet (254 nm) to the h-line (405 nm), enabling high-efficiency and high-resolution patterning with a minimum pixel size of 2 μm. The patterned QD film retained approximately 90% of its pristine PLQY with an improvement of over 30% in PLQY retention compared to samples patterned upon deep UV irradiation.

4.1.2 Energy alignment. After photochemical crosslinking patterning, reacted crosslinker molecules remain in the patterned QD film, thereby influencing charge transport and recombination processes in QDs. The highest occupied molecular orbital (HOMO) and lowest unoccupied molecular orbital (LUMO) of crosslinkers should reside outside the conduction and valence bands of QDs, thus avoiding introduction of additional electron or hole traps and minimizing adverse effects on charge carrier transport and recombination (Scheme 3d). Recently, Tang's research team engineered bisazide crosslinkers that incorporate a rigid cyclopentane bridge (Fig. 4a, bottom).[70] This structural rigidity effectively raises the LUMO of the bisazides and consequently unwanted electron transfer from the QDs to the crosslinkers is suppressed, leading to enhanced performance in the final QLED device.

4.1.3 Main reaction rate. A high main reaction (*e.g.*, C–H insertion for nitrenes and carbenes) rate is a critical design criterion for crosslinkers. Here, we take nitrene- and carbene-based crosslinkers as examples (Fig. 3b). Singlet nitrene intermediates (^{1}PN) adopt an open-shell ($\sigma^1\pi^1$) electronic configuration, with two unpaired electrons occupying different p orbitals with opposite spins. In contrast, singlet carbene intermediates (^{1}PC) preferentially adopt a closed-shell (σ^2) configuration, where the two electrons occupy the same p orbital with opposite spins. This electronic configuration difference endows carbene intermediates with an empty p-π orbital capable of accommodating new electron pairs, thereby promoting C–H insertion. According to previous studies, the C–H insertion rate of carbenes is 2−3 orders of magnitude higher than that of nitrenes.[71,72] This allows carbene-based crosslinkers to effectively achieve QD patterning even with relatively low molar absorption. Another strategy to improve main reaction efficiency is to endowing multiple crosslinkable units in photocrosslinkers (Scheme 3e). For effective crosslinking, each crosslinker must activate at least two photoactive units. The nitrene-based IP-6-LiXer, containing six azide units per molecule, significantly enhances the probability of multi-unit activation, enabling efficient QD crosslinking at reduced dosages

(Fig. 4a, top left).[33] This design facilitates effective patterning under ultralow UV exposure while minimizing loss in PLQY. At a film-thickness retention ratio of ≈80%, IP-6-LiXer preserves nearly complete PLQY in InP/ZnSeS QD films, whereas the 2-LiXer featuring only two azide units per molecule retains only ≈65%. Similar principle applies to carbene-based crosslinkers. When exposed to 365 nm light at a dose of 100 mJ cm^{-2}, Tris-TAD crosslinkers—which contain three diazirine units per molecule—achieve a film retention ratio of 80%. In contrast, O-TAD or E-TAD crosslinkers, each with only two diazirine units per molecule, reach a retention ratio of only 60%.[36]

4.1.4 Side reactions. Occurrence of side reactions also compromises crosslinking efficiency and could adversely affects luminescent properties of QDs. Here, side reactions refer to unintended chemical pathways that compete with the desired crosslinking process. These reactions may either consume the crosslinker without contributing to covalent crosslinking or generate reactive intermediates/byproducts that subsequently interact with the surface sites of QDs (Scheme 3f). As for nitrene-based crosslinkers, the photogenerated nitrene intermediates may convert into Lewis acidic byproducts such as azo-compounds and aromatic amines *via* side reactions.[72] These byproducts readily react with surface ligands (*e.g.*, oleylamine, thiols), leading to ligand loss and introduction of surface defects in QDs.[73] Moreover, Fourier transform infrared (FTIR) characterization revealed that the decline in PLQY of QDs during nitrene-based patterning coincides with extensive generation of nitrene intermediates.[35] This indicates that excess nitrene intermediates not only undergo C–H insertion but also attack QD surface sites, introducing non-radiative recombination defects. To address this issue, Kang group introduced sterically bulky isopropyl groups—to lower the probability of nitrene interactions with the QD surface, thus mitigating the formation of photochemical defects (Fig. 4a, left).[33]

In contrast, carbene intermediates, due to high energy barriers, are less prone to such side reactions. Carbene-based ligands have been reported to effectively passivate the QD surfaces, thereby maintaining the optical properties of QD films throughout the patterning process.[74,75] Although carbene-based crosslinkers do not produce harmful byproducts, their propensity for side reactions with oxygen substantially limits their practical applicability in QLED manufacturing. As shown in Fig. 3b, singlet carbene intermediates (^{1}PC) are generated upon UV irradiation and further undergo C–H insertion between surface ligands to achieve patterning of QDs. Nevertheless, due to the small singlet–triplet energy gap, ^{1}PC undergoes rapid intersystem crossing to the triplet state (^{3}PC). The resulting ^{3}PC is readily quenched by oxygen ($^3O_2$). In ambient air, this side reaction becomes the dominant pathway, which depletes the ^{1}PC population and leads to an unacceptably low efficiency of the C–H insertion reaction. The results of DFT calculations, Hammett substituent parameter analysis, and electron paramagnetic resonance (EPR) experiments revealed that introducing electron-donating groups (EDGs) at the *para*-position of the diazirine moiety effectively lowers the energy of ^{1}PC and induces an inversion of the singlet-triplet energy (Fig. 4b).[36] Consequently, ^{3}PC becomes the excited state, which means the photogenerated ^{1}PC no longer readily converts to the oxygen-sensitive ^{3}PC. Instead, it preferentially undergoes the desired C–H insertion reaction for QD patterning. Based on this mechanism, carbene-based crosslinkers functionalized with electron-donating alkoxy substituents were designed. This enabled the nondestructive patterning of both Cd-based and Cd-free QD films under 365 nm irradiation in an ambient atmosphere, without compromising their optoelectronic performance.

The discussions of above principles primarily use nitrene- and carbene-based crosslinkers as examples. However, these outlined principles and chemical modification strategies are also applicable to other types of crosslinkers. Based on DFT-guided design, Kang and co-workers structurally engineered benzophenone-based crosslinkers by substituting EDGs (–$N(CH_2)_4$ and –S–) at the *para*-positions. This modification resulted in a red-shifted absorption into the UV-A region and a significantly enhanced extinction coefficient from 60 M^{-1} cm^{-1} to 2.02 × 10^4 M^{-1} cm^{-1} at 365 nm.[34] As for design of thiol-based crosslinkers, guided by DFT calculations, Lee and co-workers revealed that conjugation extension could enhance orbital overlap and reduce the bandgap of the crosslinker, leading to improved charge transport within the QD film. Meanwhile, frontier energy-level alignment lowers the injection barrier between the crosslinker and the QDs by matching their HOMO/LUMO levels, thereby facilitating efficient carrier injection. Together, these two design strategies synergistically preserve the PLQY while substantially boosting the EL efficiency of the resulting devices, as evidenced by the higher EQE achieved with BPDT-based crosslinkers compared to TBBT-based ones.[65] Moreover, as demonstrated in the work of Cho's group, systematic molecular engineering—including the selection of dithiol functionalities, optimization of alkyl chain length, and modulation of polarity—led to the design of ODT and DDT as efficient thiol crosslinkers. Their tailored structure ensures high colloidal stability in formulated inks, enables effective liquid-crystal-assisted patterning, and promotes photocatalytic crosslinking under low UV doses.[66]

4.2 State-of-the-art of direct photopatterned QLEDs using photocrosslinkers

Based on the systematic understanding of molecular design principles and optimization strategies for crosslinkers, research has progressively advanced toward developing designs of crosslinkers that are better aligned with luminescent properties of QDs and their practical application requirements. This progress has enabled photocrosslinking-based patterned QLEDs to achieve significant performance enhancements, gradually approaching state-of-the-art non-patterned device performance. The latest advancements have further applied these photocrosslinking patterning techniques to QLED fabrication, successfully realizing high-performance patterned devices (Table 1).

4.2.1 Patterned II–VI QLEDs. Kang, Bae, and co-workers have utilized EBT nitrene-based non-specific crosslinkers to construct red-emitting CdSe/CdZnSe/ZnSeS patterned QLED,

Table 1 Reported device characteristics for patterned QLEDs[a]

Photochemistries	QDs (color)	L_{max} (cd m^{-2})	EQE_{max}	CE_{max} (cd A^{-1})	Lifetime (h)	Ref.
Patterned II–VI QLEDs						
PTPA-N_3-SH crosslinkable ligands	CdSe/ZnCdS (R)	11 720	6.3%	5.7	N/A	59
MMPE/MEMA/MMES crosslinkable ligands	CdSe/ZnS (R)	10^4–10^5	22.0%	N/A	N/A	61
	CdSe/ZnS (G)	10^4–10^5	14.4%			
	CdSe/ZnS (B)	10^3–10^4	11.4%			
Dual ligands (benzophenone)	CdSe/CdZnSe/ZnSeS (R)	$\approx 10^5$	$\approx$20%	N/A	N/A	34
	CdSe/CdZnSe/ZnSeS (G)	$\approx 10^5$	$\approx$15%			
Dual ligands (TPP)	CdSe/ZnS (R)	15 103	20.2%	25.1	T_{95}@1 k = 9280	38
	CdSe/ZnS (G)	57 326	25.6%	94.7	T_{95}@1 k = 18 261	
	CdSe/ZnS (B)	7472	21.6%	12.5	T_{95}@1 k = 135	
Dual ligands (diazirines)	CdZnSe (R)	99 369	10.3%	N/A	N/A	63
Dual ligands (azobenzene)	CdZnSe/CdZnS/ZnS (R)	$\approx 3 \times 10^3$	8.2%	N/A	T_{95}@1 k = 970	102
Nitrene-based crosslinkers	CdSe/CdZnSe/ZnSeS (R)	10^5–10^6	14.6%	N/A	T_{95}@10 k = 10	55
	CdSe/CdZnSeS (G)	$\approx 10^5$	$\approx$6%		N/A	
	CdZnS/ZnS (B)	10^3–10^4	$\approx$3%		N/A	
Nitrene-based crosslinkers	CdZnSe/CdZnS/ZnS (R)	6693	12.6%	N/A	T_{95}@1 k = 1823	32
Rigid nitrene-based crosslinkers	CdSe QDs (R)	179 872	21.1%	23.3	T_{95}@10 k = 3.1	70
	CdSe QDs (G)	244 884	9.6%	40.9	N/A	
	CdSe QDs (B)	4939	$\approx$2%	1.47	N/A	
Carbene-based crosslinkers	CdZnSe/CdZnS/ZnS (R)	11 300	11.7%	N/A	T_{95}@1 k = 4852	32
Benzonphenone-based crosslinkers	CdSe/ZnS (R)	109 879	16.5%	N/A	T_{95}@1 k = 2258	76
Azide-alkyne click chemistry	CdZnSe/ZnSe (R)	166 612	20.1%	N/A	T_{95}@1 k = 582	40
	CdSe/ZnSe/ZnS (G)	10^5–10^6	15.4%		N/A	
	CdZnSe/ZnSe/ZnS (B)	10^4–10^5	8.5%		N/A	
Azide-alkyne click chemistry*	CdZnSe/ZnSe (R)	10^4–10^5	$\approx$9%	N/A	N/A	40
	CdSe/ZnSe/ZnS (G)	$\approx 10^5$	$\approx$6%			
	CdZnSe/ZnSe/ZnS (B)	$\approx 10^4$	$\approx$3%			
Patterned III–V QLEDs						
Dual ligands (FPA-S)	InP/ZnSe/ZnS (R)	10^5–10^6	N/A	4.3	T_{95}@150 = 950	64
Nitrene-based crosslinkers	InP/ZnSeS (G)	$\approx$4000	8.3%	N/A	T_{90}@1k = 156	33
EDG-modified carbene-based crosslinkers	InP/ZnSe/ZnS (R)	39 590	15.3%	20.2	N/A	36
EDG-modified carbene-based crosslinkers*	InP/ZnSe/ZnS (R)	$\approx$4000	13.3%	20.8	N/A	36
Thiol-ene click chemistry	InP/ZnS (G)	8463	N/A	23.0	N/A	62
Patterned perovskite NC LEDs						
Dual ligands (methacrylate)	$CsPbBr_3$ (G)	51 181	18.6%	N/A	T_{50} = 1.95	77
Dual ligands (acrylate)	$CsPbBr_3$ (G)	<100	1%	N/A	N/A	86
Nitrene-based crosslinkers	$FAPbBr_3$ (G)	20 900	6.8%	28.5	N/A	35
	$CsPbBr_3$ (G)	1929	1.8%	5.6		
Carbene-based crosslinkers	$FAPbBr_3$ (G)	64 726	16%	60	T_{50}@100 = 26	37
Thiol-ene click chemistry	$CsPbBr_3$ (G)	$\approx$100	$\approx$2.5%	N/A	N/A	56
Thiol-ene click chemistry*	$CsPbBr_3$ (G)	29 968	13.1%	N/A	N/A	78

[a] Contents marked with * represents data measured from pixelated QLEDs. Device performance is co-determined by materials chemistry (QDs, ligands, crosslinkers) and device engineering (charge transport layers, interfaces, device architecture) and thus emphasizing performance improvement within the same method is more meaningful than making absolute comparisons across different methods and device systems.

achieving a EQE_{max} of 14.6% (Fig. 5a).[55] This marks the first reported achievement of an EQE exceeding 10% in patterned QLEDs. Furthermore, they successfully fabricated red and green dual-colour pixelated QLED with a minimum pixel size of 10 × 38 μm. Zhang group demonstrated that the choice of photo-crosslinkers determined the EL performance of patterned QLEDs. Using red-emitting CdZnSe/CdZnS/ZnS devices as a case study, devices patterned with carbene-based crosslinkers maintained identical EQE and operational lifetime with non-patterned devices, achieving an EQE of about 12%, while those patterned with nitrene-based crosslinkers showed degradation in both performance metrics (Fig. 6a).[32] More recently, Tang group designed bisazide crosslinkers featuring a rigid cyclopentane moiety. The rigidity of this linker elevates the LUMO level of the bisazides, which suppresses electron transfer from QDs to the crosslinker and enhances device performance. As a result, red-emitting CdSe-based patterned QLEDs fabricated with these crosslinkers achieved a EQE_{max} of about 21% and L_{max} approaching 18 000 cd m^{-2}.[70]

As for specific crosslinkers, Lee's group employed BPDT based on thiol-ene click chemistry to fabricate high-performance patterned CdSe-based QLEDs.[65] The resulting devices retained the intrinsic optoelectronic properties of the QDs while achieving an EQE_{max} of 9.73% and a high luminance

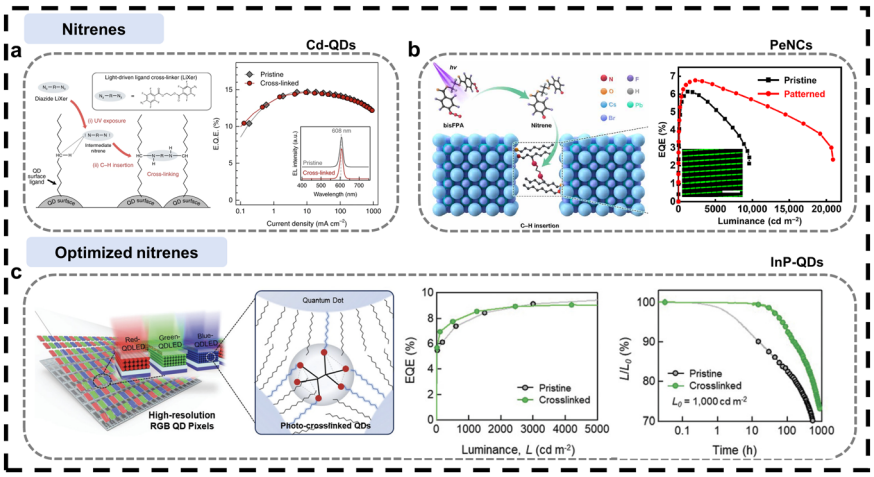

Fig. 5 Representative examples of patterned QLEDs achieved by nitrene-based crosslinkers. (a) Cd-based patterned QLED *via* nitrene-based crosslinkers.[55] Adapted with permission from ref. 55. Copyright 2020 Springer Nature. (b) $CsPbBr_3$ LED *via* nitrene-based crosslinkers.[35] Adapted with permission from ref. 35. Copyright 2022 American Association for the Advancement of Science. (c) InP-based patterned QLED *via* structurally optimized nitrene-based crosslinkers.[33] Adapted with permission from ref. 33. Copyright 2022 Wiley-VCH.

of 10, 000 cd m^{-2}. Notably, the current efficiency and power efficiency of the BPDT-patterned QLEDs were nearly identical to those of the non-patterned reference devices, demonstrating that this crosslinking strategy enables high-resolution patterning without compromising device performance. Besides, Zhang and colleagues developed red, green, and blue monochromatic patterned QLEDs based on the light-triggered azide-alkyne cycloaddition reaction.[40] In this system, 10-undecynoic acid was used as the alkyne-functionalized photosensitive ligand to replace native oleic acid, while 4,4′-bis(azidomethyl)biphenyl served as the photocrosslinkers. The resulting patterned devices outperformed their non-patterned counterparts, achieving a EQE_{max} of 20.05% (red, CdZnSe/ZnSe), 15.37% (green, CdSe/ZnSe/ZnS), and 8.49% (blue, CdZnSe/ZnSe/ZnS), compared to 18.15%, 14.15%, and 7.02% for the corresponding prototype devices, respectively.

Similarly, dual-ligand strategy has also enabled high-performance patterned QLEDs. Hahm *et al.* constructed patterned QLEDs using dual-ligand $CdSe/Cd_xZn_{1-x}Se/ZnSe_ySy_{-1}$ QDs, achieving device performance comparable to that of prototype devices with an EQE_{max} of approximately 20% (Fig. 7c).[34] Furthermore, they fabricated a 10 × 10 passive matrix full-colour RGB display prototype (PM-QLED), demonstrating the practical application potential of this patterning method in the field of optoelectronic displays (Fig. 8a). In recent work, Lee and colleagues employed TDBA as PXLs.[63] Using this bifunctional molecule, high-resolution (≈2 μm) CdZnSe-based patterned QLEDs were successfully fabricated, achieving a L_{max}

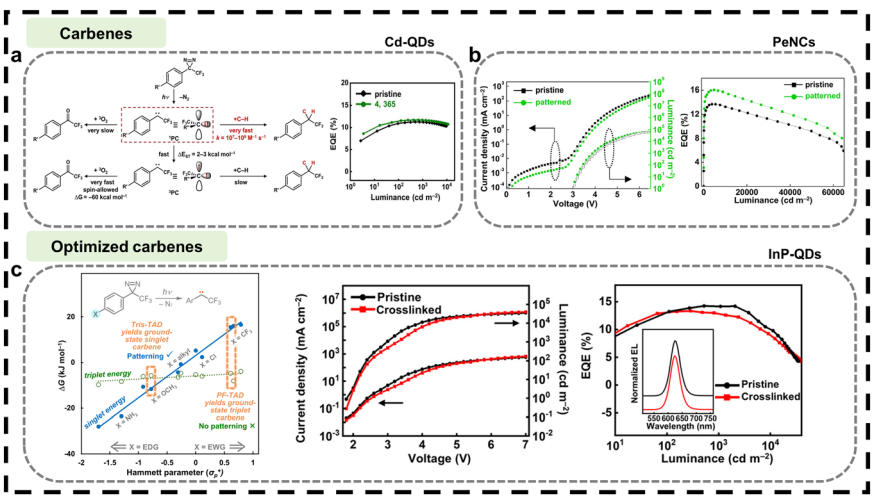

Fig. 6 Representative examples of patterned QLEDs achieved by carbene-based crosslinkers. (a) Cd-based QLED *via* carbene-based crosslinkers under inert atmosphere.[32] Adapted with permission from ref. 32. Copyright 2022 Wiley-VCH. (b) $FAPbBr_3$ LED *via* carbene-based crosslinkers under inert atmosphere.[37] Adapted with permission from ref. 37. Copyright 2024 American Chemical Society. (c) InP-based QLED *via* electronically optimized carbene-based crosslinkers under ambient atmosphere.[36] Adapted with permission from ref. 36. Copyright 2024 American Chemical Society.

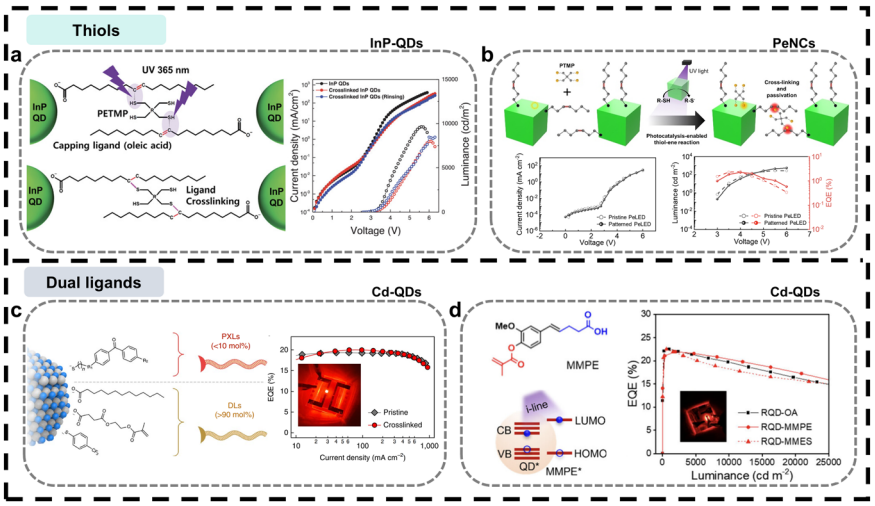

Fig. 7 Representative examples of patterned QLEDs achieved by thiol-based crosslinkers and dual ligand strategy. (a) InP-based QLED *via* thiol-based crosslinkers.[62] Adapted with permission from ref. 62. Copyright 2023 Wiley-VCH. (b) $CsPbBr_3$ LED *via* thiol-based crosslinkers.[56] Adapted with permission from ref. 56. Copyright 2023 American Association for the Advancement of Science. (c and d) Cd-based QLEDs *via* dual ligand strategy.[34,61] Adapted with permission from ref. 34 and 61. Copyright 2022 Springer Nature and 2025 American Chemical Society.

of 99 369 cd m^{-2} and a peak EQE of 10.3%. These results demonstrate the effectiveness of TDBA-based ligand design for producing high-performance patterned QLEDs. The Wang group developed red-emitting patterned QLEDs using methacrylate-anchored CdSe/ZnS QDs that are processable in the industry-standard solvent PGMEA, achieving a peak EQE of 22% and a L_{max} exceeding 40 000 cd m^{-2} (Fig. 7d).[61] More recently, they reported another strategy using TPP ligand as photoinitiator to initiate a chain-propagation reaction, leading to the crosslinking of the QDs. The resulted red-, green-, and blue-emitting CdSe/ZnS patterned QLED achieves EQE_{max} of 20.2%, 25.6%, and 21.6% respectively.[38] As shown in Fig. 8c, this method was further demonstrated in fabrication of an active-matrix QD display prototype (AM-QLED).

Photocrosslinking approach is also a compatible patterning method for charge-transport layers in devices. For instance, Li *et al.* fabricated full-color pixelated CdSe-based QLEDs with an EQE of 11% by combining a region-selective assembly process with photocrosslinking lithography, using the nitrene-based crosslinker 4,4′-dithiobis(phenylazide).[26] Instead of patterning QD films, Zhang also presented an alternative strategy of creating high-quality photocrosslinked TFB films with ordered molecular arrangement using a nitrene-based crosslinker 2,6-bis(4-azidobenzylidene)-4-methylcyclohexanone (AMBK).[19] Red-emitting CdSe/ZnS QLED devices incorporating the photocrosslinked TFB layers demonstrated significantly enhanced performance, achieving an EQE_{max} of 24.6% and a current efficiency (CE) of 24.3 cd A^{-1}. The device lifetime (T_{95}) was markedly improved from 460 to 1256 hours. Furthermore, the feasibility of this approach was also demonstrated by the successful fabrication of pixelated QLED devices using patterned TFB layers.

4.2.2 Patterned III–V QLEDs. The development of cadmium-free QLED devices is important due to their low toxicity, environmental compatibility, and alignment with global sustainability goals. However, achieving high performance in such systems remains challenging, as the photochemical processes required for direct patterning, including UV exposure and the generation of reactive intermediates such as radicals or protons, can induce photo-oxidation, introduce surface defects, and degrade the optical and electrical properties of QDs. These adverse effects are particularly pronounced in chemically more fragile heavy-metal-free QDs, thereby constraining the EQE of patterned III–V QLEDs to values generally below 10%.[69,79,80] Overcoming these material and process-related vulnerabilities is therefore essential for advancing the practical performance of cadmium-free QLED technologies.

Kang group developed structurally optimized nitrene-based non-specific crosslinkers IP-6-Lixer to construct green-emitting InP/ZnSeS patterned devices, with an EQE_{max} of 8.3% and a luminance over 1000 cd m^{-2} (Fig. 5c).[33] Oh group utilized thiol-based specific crosslinkers PTMP to build InP/ZnSe/ZnS patterned devices *via* a thiol-ene reaction (Fig. 7a).[62] The resulted devices achieved a L_{max} of 8463 cd m^{-2} and a peak current efficiency of 23 cd A^{-1}. Besides, Seo *et al.* has utilized FPA-S as PXLs to successfully fabricate red-emitting InP/ZnSe/ZnS patterned QLED featuring a CE_{max} of 4.3 and a L_{max} over 10^5–10^6 cd m^{-2}.[64]

Recently, our group developed electronically optimized carbene-based crosslinkers, Tris-TAD, which are activated by i-line UV irradiation to generate air-stable singlet carbenes that directly link adjacent QDs *via* concerted C–H insertion into the surface ligands. The fabricated InP/ZnSe/ZnS patterned QLEDs achieved a EQE_{max} of 15.3% and L_{max} over 39 590 cd m^{-2}, establishing a record performance for patterned InP-based QLEDs (Fig. 6c).[36] Based on this method, we further fabricated an AM-QLED using Tris-TAD (Fig. 8b). The InP-based QD film was integrated with a pixelated thin-film transistor (TFT) array (backplane: 16 × 16 TFT array), where each patterned QD film was aligned precisely with its underlying TFT. This architecture

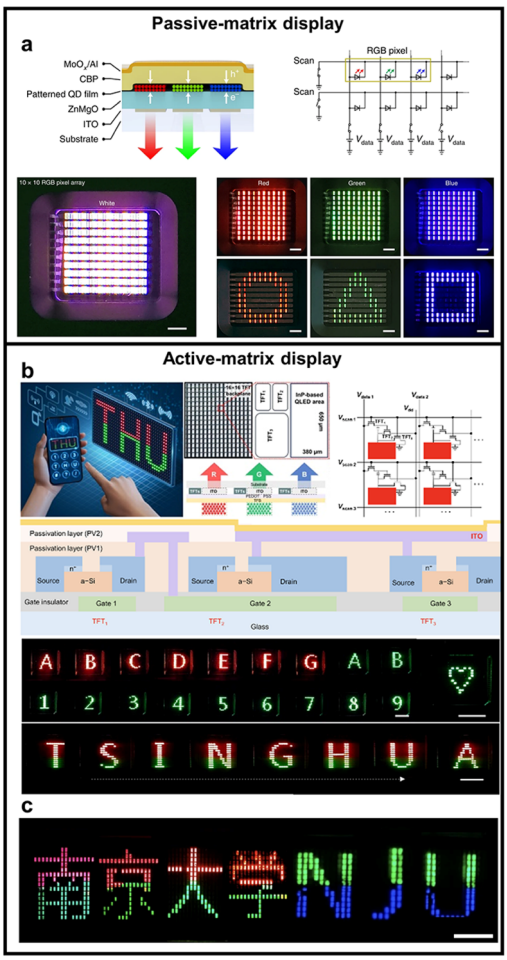

Fig. 8 Active- and passive-matrix displays of photocrosslinked QD patterns. (a) PM-QLED of CdSe-based QDs *via* dual ligands.[34] Adapted with permission from ref. 34. Copyright 2022 Springer Nature. (b) AM-QLED of InP-based QDs *via* carbene-based crosslinkers.[36] Adapted with permission from ref. 36. Copyright 2024 American Chemical Society. (c) AM-QLED of RGB QDs *via* TPP ligands.[38] Adapted with permission from ref. 38. Copyright 2025 Springer Nature.

enabled precise selective control of charge injection into individual pixels (size: 380 × 650 μm) *via* Bluetooth from a mobile device, without interference from adjacent pixels or leakage current. Importantly, the performance of individual pixels of AM-QLED was also characterized, exhibiting a CE of 20.8 cd A^{-1} and an estimated peak EQE of 13.3%. These values closely match those obtained from QLED devices based on full crosslinked film. This consistency of pixel-level device has validated the technical feasibility of a transition path for QD-integrated devices to industrial applications.

4.2.3 Patterned perovskite NC LEDs. Perovskite NCs have emerged as highly promising optoelectronic materials owing to their unique properties.[81–83] However, the development of patterned perovskite devices faces distinct and severe challenges that are not encountered in conventional II–VI or III–V QD systems. The ionic nature of perovskite NCs makes them exceptionally sensitive to polar solvents, limiting the choice of processable inks and complicating multilayer integration. Besides, their fragile crystal structures are prone to degradation under mild air and moisture, as well as phase transitions triggered by temperature fluctuations or chemical perturbations.[84,85] Furthermore, perovskite NCs exhibit pronounced photo- and chemo-instability. UV exposure and photogenerated species during patterning can accelerate ion migration, induce surface defects, and quench luminescence. Consequently, many crosslinking strategies successful for II–VI or III–V QDs cannot be directly transferred to perovskite systems. In this context, photocrosslinking-based approaches have attracted growing research attention due to their potential for benign processing and pattern fidelity, leading to notable progress in patterned perovskite NCs light-emitting diodes (PeLEDs) in recent years.

In 2022, our group has developed DOPPLCER method using nitrene-based crosslinkers for perovskite NCs patterning and further demonstrated patterned PeLEDs employing $CsPbBr_3$ which established then-record performance metrics with an EQE_{max} of 6.8% and L_{max} over 20 000 cd m^{-2} (Fig. 5b).[35] To further enhance the performance of PeLEDs, we employed carbene-based crosslinkers to fabricate patterned $FAPbBr_3$ PeLEDs (Fig. 6b).[37] These devices achieved an EQE_{max} of 16% and a L_{max} over 60 000 cd m^{-2}, representing a significant improvement over counterparts patterned using nitrene-based crosslinkers. The results underscore the milder reactivity and enhanced compatibility of carbene-based crosslinking with fragile perovskite NCs.

Maeng *et al.* presented a photocatalytic patterning method based on thiol-ene click reaction to fabricate $CsPbBr_3$ patterned LED, achieving EQE_{max} of ≈2.5% and L_{max}≈100 cd m^{-2} (Fig. 7b).[56] More recently, they reported a dual strategy combining ligand re-engineering and anion exchange to achieve high-performance patterned PeLEDs.[66] High-resolution, nondestructive photocatalytic patterning was first realized using optimized thiol-based crosslinkers (ODT/DDT), followed by a film-state ligand-exchange process that further enhanced the optoelectronic properties of the patterned films. As a result, green $CsPbBr_3$ patterned devices reached a peak EQE of 14.7% with a luminance of ≈25 400 cd m^{-2}, while red $CsPbBr_xI_{3-x}$ patterned devices achieved an EQE exceeding 13.1%, marking the first demonstration of directly photopatterned red perovskite LEDs.

5 Extension of photocrosslinking to other types of nanomaterials and 3D printing

Beyond QDs, photocrosslinking-enabled patterning also provides an effective pathway for the patterning of other types of nanomaterials, such as MOFs, and offers viable solutions for 3D printing of inorganic nanomaterials.

5.1 Direct photopatterning of MOFs

MOFs are a class of porous crystalline materials formed by the self-assembly of metal ions/clusters and organic linkers. They possess exceptional surface areas, tuneable pore architectures, and compositional diversity.[87] These properties have spurred

their recent adoption in microelectronics and nanophotonics.[88–90] Integrating photocrosslinking chemistry with colloidal MOFs processing, we developed a universal methodology for patterning MOFs (CLIP-MOF).[91] This technique enables large-area (*e.g.*, 4-inch wafer) patterning of diverse MOFs (including ZIF-8, ZIF-7, HKUST-1, and UiO-66) with micro-to nanoscale resolution (≈5 μm with UV; ≈70 nm with electron-beam lithography) on rigid and flexible substrates, in both single- and multi-component configurations (Fig. 9a).

The mechanism of CLIP-MOF is similar with direct photopatterning of QDs: both exploit photo-induced changes in colloidal stability. Alternatively, the inherent chemical lability of MOFs towards stimuli like acids, bases, or water can also be harnessed for direct lithography. Leveraging this, Tu group introduced a method using photoacid generators (PAGs).[92] UV exposure liberates protons from PAGs, which subsequently decompose the MOFs in irradiated areas—functioning as a positive-tone photoresist—to yield patterns with a resolution of ≈2 μm while preserving the material's intrinsic properties. Our group devised a complementary, negative-tone strategy based on photo-induced fluorination of zeolitic imidazolate frameworks (ZIFs) using methyl 4-azido-2,3,5,6-tetrafluorobenzoate (ATFB).[93] Rather than destructively decomposing MOFs with high-dose radiation, this method uses an ultra-low dose (254 nm, 10 mJ cm^{-2}) to covalently graft ATFB onto the ZIF ligands. This fluorination enhances the water stability of the exposed regions, allowing the unexposed, pristine ZIFs to be developed away with water/ammonia solution (Fig. 9b). This technique is generalizable across several water-labile ZIFs (ZIF-8, ZIF-7, ZIF-67, ZIF-L), achieving feature sizes of ≈2 μm.

Critically, these direct lithographic methods maintain the structural integrity, chemical composition, and porosity of the original MOFs. The resulting patterned MOF films show promise for transformative applications in diffraction-based

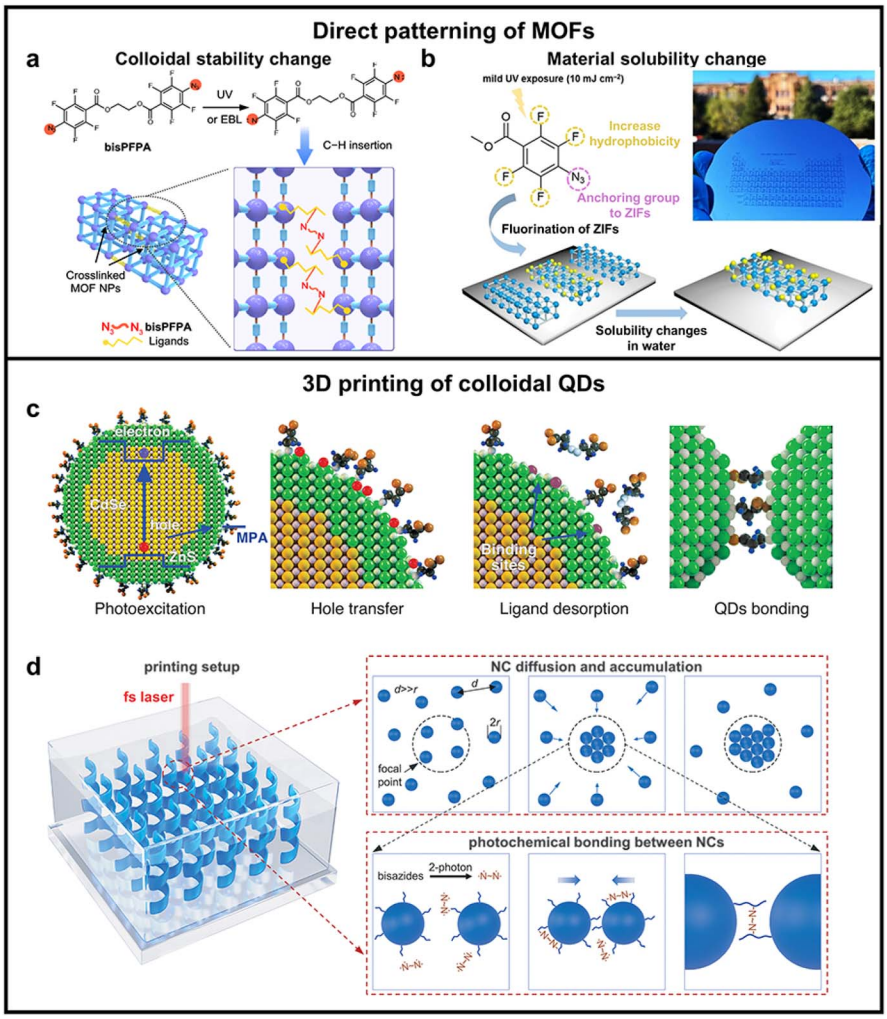

Fig. 9 Photocrosslinking chemistries in patterning of colloidal MOFs and 3D nanoprinting of QDs. (a) Direct patterning of MOFs *via* nitrene-based crosslinkers.[91] Adapted with permission from ref. 91. Copyright 2024 Springer Nature. (b) Direct patterning of ZIFs *via* photoinduced fluorination.[93] Adapted with permission from ref. 93. Copyright 2025 Wiley-VCH. (c and d) 3D printing of QDs *via* PEB (c) and 3D Pin (d).[99,100] Adapted with permission from ref. 99 and 100. Copyright 2022 American Association for the Advancement of Science and 2023 American Association for the Advancement of Science.

gas sensing, pixelated electrochromic devices, fluorescent sensor arrays, information encryption, and intelligent, multiplexed sensing platforms.

5.2 3D nanoprinting of QDs

3D printing is a transformative fabrication technology that enables the creation of complex three-dimensional structures with customizable material compositions, thereby unlocking new functionalities across advanced fields such as aerospace, energy materials, bioengineering, and personalized manufacturing.[94–97] Particularly, the introduction of femtosecond laser-based techniques has pushed the resolution into the nanoscale, allowing the fabrication of intricate 3D architectures with nanoscale precision and unprecedented functional integration.

Semiconductor inorganic materials are indispensable in integrated circuits and photonic chips due to their superior optoelectronic properties. The ability to 3D print semiconductors and other inorganics could offer a viable pathway for out-of-plane processing of integrated chips. However, current 3D printing is largely confined to polymers and metals, lacking effective methods for micro/nano-scale printing of semiconductors and many other inorganic materials.[98] To address this challenge, Liu *et al.* presented a strategy termed photoexcitation-induced chemical bonding (PEB), which utilizes electron–hole pairs generated by photoexcitation to modify QD surface chemistry and further trigger interparticle chemical bonding (Fig. 9c).[99] In this process, mercaptopropionic acid (MPA) ligands are attached to CdSe/ZnS core/shell QDs *via* thiol coordination, leaving their carboxylic acid groups exposed to the solvent. When irradiated with a femtosecond laser at 780 nm through two-photon absorption, the excited QDs produce charge carriers whose energy levels promote the oxidation and removal of the bound MPA ligands. The newly created coordination-deficient sites on the QD surface then selectively bind to carboxylate terminals from MPA ligands anchored on adjacent QDs, forming robust inter-dot bridges that lock the assembly into a precise 3D network. As a result, high-accuracy, high-resolution 3D structures (feature sizes down to 80 nm) of QDs with photonic properties maintained were achieved using this method.

Furthermore, Li *et al.* has leveraged photo-crosslinking chemistry to develop a universal 3D printing method for inorganic nanomaterials (3D Pin).[100] The 3D Pin process employs NC solutions as inks, into which an azide-based crosslinker is incorporated. Under femtosecond laser irradiation, the decomposition of the crosslinker generates nonspecific C–H insertion reactions, leading to covalent crosslinking between the organic ligands capping the NCs (Fig. 9d). The non-specificity of the nitrene intermediate insertion renders this method universally applicable to diverse materials, including semiconductors (*e.g.*, II–VI, III–V, metal halide perovskites), metals (*e.g.*, Au), and metal oxides (*e.g.*, In_2O_3, TiO_2). Furthermore, by blending different NC solutions, hybrid tetrahedral structures comprising CdSe/ZnS, TiO_2, PbS/CdS, and In_2O_3 have been successfully printed. The 3D Pin technique achieves nanoscale resolution (≈150 nm), enabling the fabrication of arbitrarily complex 3D architectures. The printed structures exhibit a high inorganic mass fraction of approximately 90%, paving a promising fabrication route for applications in 3D holographic displays and integrated 3D optoelectronic devices.

6 Conclusion and outlook

6.1 Conclusion

This review surveys the progress of photocrosslinking chemistry for directly patterning colloidal QDs. We focus on the key design principles driving this field toward a critical application of high-performance, pixelated QLEDs. The evolution from simple proof-of-concept to advanced patterning methods is rooted in a deeper understanding of the underlying photochemistry. The field now recognizes that the molecular design of ligands and crosslinkers must achieve dual objectives: ensuring high-resolution patterning while preserving the optoelectronic properties of the QDs. This dedicated focus on "nondestructive" photocrosslinking chemistry has contributed to the successful fabrication of patterned QLEDs with continuously improving optoelectronic performance. These encouraging advances suggest the great promise of photocrosslinking-based approaches for incorporating QDs into integrated optoelectronic platforms, such as high-resolution displays and advanced photonics.

6.2 Outlook

6.2.1 From the application perspective. Looking forward, the field of direct photopatterning *via* photocrosslinking is poised to transition from laboratory-scale demonstrations toward integrated system fabrication and practical manufacturing for high-resolution display. Several key challenges, however, must be addressed. The fabrication and performance evaluation of fully pixelated devices, such as high-resolution QLED displays, will be a critical milestone, moving to functional pixelated displays.[20,21] In this endeavour, mitigating issues like current leakage between adjacent pixels remains a priority, as such leakage becomes increasingly severe with diminishing pixel sizes. It is worth noting that in high-resolution architectures, leakage issues are often exacerbated by the absence of a robust pixel define layer (PDL) and insufficient process compatibility between crosslinked QD layers and

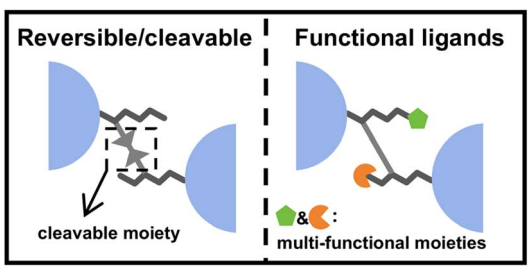

Scheme 4 Ligands modified with reversible/cleavable or functional moieties.

conventional PDL materials. Unlike inkjet printing, where bank structures inherently define the pixelated architecture, many photolithography-based patterning studies focus solely on thin film devices without integrating these critical PDL components to achieve fully pixelated displays. To address this issue, future research could focus not only on novel patterning chemistries but also on the integration of insulating barriers. Promising strategies have recently been demonstrated, including the incorporation of honeycomb-patterned insulating PMMA films to separate charge transport layers,[101] the introduction of fluorosilane (PFTS) barriers between pixels *via* electrostatic force-induced deposition,[102] and the use of an ultrathin photoresist layer (20 nm)[103] or lithographically patterned SiO_2 insulating layers[104] to suppress current leakage. These examples underscore that advancing PDL materials and integration strategies capable of coexisting with crosslinked QD films represents a promising pathway to suppress leakage current and enhance the performance of next-generation pixelated displays. Key considerations include ensuring solvent resistance of the QD layer during PDL processing, controlling surface energy for defect-free PDL coating, and matching thermal budgets. Advancing PDL materials and integration strategies that can coexist with crosslinked QD films represents a promising path to suppress leakage and enhance performance of pixelated devices. Furthermore, achieving compatibility with established industrial workflows is indispensable for large-scale adoption.[105] This necessitates a shift toward environmentally benign and process-compatible solvents, moving beyond the conventional, often hazardous solvents used in research labs. Finally, the molecular design of photocrosslinkers and ligands is inherently complex. Here, artificial intelligence-assisted computational screening and optimization may serve as powerful tools to accelerate the discovery of next-generation crosslinkers with tailored properties, such as high photosensitivity and reactivity and minimal impact on QD luminescence. The successful convergence of these parallel efforts—in device engineering, industrial compatibility, and data-driven material science—is expected to play a decisive role in advancing the commercial viability and broadening the technological impact of direct photocrosslinking patterning.

6.2.2 From the chemistry perspective. There are several research directions with the potential to deepen the fundamental understanding and expand the functional utility of direct photopatterning. Firstly, moving beyond qualitative demonstrations toward a more rigorous quantitative framework is desirable. A critical challenge lies in the limited mechanistic and quantitative understanding of the photochemical crosslinking processes involved in QD patterning. Therefore, a systematic investigation employing precise chemical characterization is imperative to establish this quantitative relationship. This entails utilizing advanced analytical techniques to accurately quantify the density of crosslinked ligands and correlate it with the corresponding alterations in the solubility of QDs. Such research is crucial for constructing predictive models that could guide the rational design of photocrosslinking chemistries. Beyond the primary goal of forming covalent bonds between ligands on neighbouring QDs, future molecular designs should explore dynamic crosslinking motifs. The introduction of reversible or cleavable bonds would enable pattern reconfigurability and facilitate device repair or recycling, adding a new dimension of versatility (Scheme 4).[106] Furthermore, moving beyond inert linkers, the strategic design of functional crosslinkers that can introduce or modulate optical and electrical properties within the patterned film presents a transformative opportunity. This shift from viewing crosslinkers as mere structural agents to utilizing them as active components could unlock novel functionalities in patterned optoelectronic devices and sensing arrays.

Author contributions

W. Q. wrote the draft and prepared figures of this review article. H. Z. supervised the preparation of the draft, edited and co-revised the manuscript.

Conflicts of interest

There are no conflicts to declare.

Data availability

No primary research results, software or code have been included and no new data were generated or analysed as part of this review.

Acknowledgements

This work was financially supported by the Beijing Natural Science Foundation (JQ24003) (H. Z.), the Natural Science Foundation of China (No. 22274087) (H. Z.), and Tsinghua University Dushi Program (H. Z.).

Notes and references

1 A. P. Alivisatos, Semiconductor Clusters, Nanocrystals, and Quantum Dots, *Science*, 1996, **271**, 933–937.
2 D. V. Talapin, J.-S. Lee, M. V. Kovalenko and E. V. Shevchenko, Prospects of Colloidal Nanocrystals for Electronic and Optoelectronic Applications, *Chem. Rev.*, 2010, **110**, 389–458.
3 M. V. Kovalenko, L. Manna, A. Cabot, Z. Hens, D. V. Talapin, C. R. Kagan, V. I. Klimov, A. L. Rogach, P. Reiss, D. J. Milliron, P. Guyot-Sionnnest, G. Konstantatos, W. J. Parak, T. Hyeon, B. A. Korgel, C. B. Murray and W. Heiss, Prospects of Nanoscience with Nanocrystals, *ACS Nano*, 2015, **9**, 1012–1057.
4 C. R. Kagan, E. Lifshitz, E. H. Sargent and D. V. Talapin, Building Devices from Colloidal Quantum Dots, *Science*, 2016, **353**, aac5523.
5 J. M. Pietryga, Y.-S. Park, J. Lim, A. F. Fidler, W. K. Bae, S. Brovelli and V. I. Klimov, Spectroscopic and Device Aspects of Nanocrystal Quantum Dots, *Chem. Rev.*, 2016, **116**, 10513–10622.

6 F. P. García de Arquer, D. V. Talapin, V. I. Klimov, Y. Arakawa, M. Bayer and E. H. Sargent, Semiconductor Quantum Dots: Technological Progress and Future Challenges, *Science*, 2021, **373**, eaaz8541.
7 A. L. Efros and L. E. Brus, Nanocrystal Quantum Dots: From Discovery to Modern Development, *ACS Nano*, 2021, **15**, 6192–6210.
8 S. Coe, W.-K. Woo, M. Bawendi and V. Bulović, Electroluminescence from Single Monolayers of Nanocrystals in Molecular Organic Devices, *Nature*, 2002, **420**, 800–803.
9 Y. Shirasaki, G. J. Supran, M. G. Bawendi and V. Bulovic,́ Emergence of Colloidal Quantum-Dot Light-Emitting Technologies, *Nat. Photonics*, 2013, **7**, 13–23.
10 X. Dai, Z. Zhang, Y. Jin, Y. Niu, H. Cao, X. Liang, L. Chen, J. Wang and X. Peng, Solution-Processed, High-Performance Light Emitting Diodes Based on Quantum Dots, *Nature*, 2014, **515**, 96–99.
11 X. Dai, Y. Deng, X. Peng and Y. Jin, Quantum-Dot Light-Emitting Diodes for Large-Area Displays: Towards The Dawn of Commercialization, *Adv. Mater.*, 2017, **29**, 1607022.
12 D. S. Dolzhnikov, H. Zhang, J. Jang, J. S. Son, M. G. Panthani, S. Chattopadhyay, T. Shibata and D. V. Talapin, Composition-Matched Molecular "Solders" for Semiconductors, *Science*, 2015, **347**, 425–428.
13 C. R. Kagan and C. B. Murray, Charge Transport in Strongly Coupled Quantum Dot Solids, *Nat. Nanotechnol.*, 2015, **10**, 1013–1026.
14 M. Yuan, M. Liu and E. Sargent, Colloidal Quantum Dot Solids for Solution-Processed Solar Cells, *Nat. Energy*, 2016, **1**, 16016.
15 X. Tang, M. M. Ackerman, M. Chen and P. Guyot-Sionnest, Dual-Band Infrared Imaging Using Stacked Colloidal Quantum Dot Photodiodes, *Nat. Photonics*, 2019, **13**, 277–282.
16 J. Kim, S.-M. Kwon, Y. K. Kang, Y.-H. Kim, M.-J. Lee, K. Han, A. Facchetti, M.-G. Kim and S. K. Park, A Skin-Like Two-Dimensionally Pixelized Full-Color Quantum Dot Photodetector, *Sci. Adv.*, 2019, **5**, eaax8801.
17 J. Yoo, K. Lee, U. J. Yang, H. H. Song, J. H. Jang, G. H. Lee, M. S. Bootharaju, J. H. Kim, K. Kim, S. I. Park, J. D. Seo, S. Li, W. S. Yu, J. I. Kwon, M. H. Song, T. Hyeon, J. Yang and M. K. Choi, Highly Efficient Printed Quantum Dot Light-Emitting Diodes through Ultrahigh-Definition Double-Layer Transfer Printing, *Nat. Photonics*, 2024, **18**, 1105–1112.
18 Q. Zhang, K. Yang, C. Luo, Z. Lin, W. Chen, Y. Yu, H. Hu and F. Li, Nanosecond Response Perovskite Quantum Dot Light-Emitting Diodes with Ultra-High Resolution for Active Display Application, *Light Sci. Appl.*, 2025, **14**, 285.
19 R. Xu, J. Fan, Z. Yao, C. Gu, Q. Nie, R. Li, J. Wang, R. J. Smith, L. Qian, C. Xiang and T. Zhang, Enhanced Molecular Stacking Enabled by Photo-Induced Crosslinking of Hole Transport Materials for High-Performance QLED, *Adv. Funct. Mater.*, 2025, e10728.
20 X. Zhang, S. Ding, Z. Tang, Z. Yao, T. Zhang, C. Xiang and L. Qian, Nanostructured Materials for Next-Generation Display Technology, *Nat. Rev. Electr. Eng.*, 2025, **2**, 263–276.
21 E.-L. Hsiang, Z. Yang, Q. Yang, P.-C. Lai, C.-L. Lin and S.-T. Wu, AR/VR Light Engines: Perspectives and Challenges, *Adv. Opt. Photonics*, 2022, **14**, 783–861.
22 C. Xiang, L. Wu, Z. Lu, M. Li, Y. Wen, Y. Yang, W. Liu, T. Zhang, W. Cao, S. W. Tsang, B. Shan, X. Yan and L. Qian, High Efficiency and Stability of Ink-Jet Printed Quantum Dot Light Emitting Diodes, *Nat. Commun.*, 2020, **11**, 1646.
23 P. Yang, L. Zhang, D. J. Kang, R. Strahl and T. Kraus, High-Rosolution Inkjet Printing of Quantum Dot Light-Emitting Microdiode Arrays, *Adv. Optical Mater.*, 2019, **8**, 1901429.
24 T.-H. Kim, K.-S. Cho, E. K. Lee, S. J. Lee, J. Chae, J. W. Kim, D. H. Kim, J.-Y. Kwon, G. Amaratunga, S. Y. Lee, B. L. Choi, Y. Kuk, J. M. Kim and K. Kim, Full-Color Quantum Dot Displays Fabricated by Transfer Printing, *Nat. Photonics*, 2011, **5**, 176–182.
25 M. K. Choi, J. Yang, K. Kang, D. C. Kim, C. Choi, C. Park, S. J. Kim, S. I. Chae, T.-H. Kim, J. H. Kim, T. Hyeon and D. H. Kim, Wearable Red-Green-Blue Quantum Dot Light-Emitting Diode Array Using High-Resolution Intaglio Transfer Printing, *Nat. Commun.*, 2015, **6**, 7149.
26 C. Zhong, K. Yu, Y. Qie, Y. Yu, Y. Lu, G. Deng, T. Guo, H. Hu and F. Li, Ultrahigh-Resolution Full-Color Quantum Dot LEDs Based on Region-Selective Interfacial Self-Assembly, *Adv. Funct. Mater.*, 2025, **35**, 2510076.
27 C. Hu, T. Aubert, Y. Justo, S. Flamee, M. Cirillo, A. Gassenq, O. Drobchak, F. Beunis, G. Roelkens and Z. Hens, The Micropatterning of Layers of Colloidal Quantum Dots with Inorganic Ligands Using Selective Wet Etching, *Nanotechnology*, 2014, **25**, 175302.
28 M. Yuan, J. Feng, H. Li, H. Gao, Y. Qiu, L. Jiang and Y. Wu, Remote Epitaxial Crystalline Perovskites for Ultrahigh-Resolution Micro-LED Displays, *Nat. Nanotechnol.*, 2025, **20**, 381–387.
29 P. Zhang, G. Yang, F. Li, J. Shi and H. Zhong, Direct *in Situ* Photolithography of Perovskite Quantum Dots Based on Photocatalysis of Lead Bromide Complexes, *Nat. Commun.*, 2022, **13**, 6713.
30 Z. Gao, J. Shi and G. Yang, Quantum Dots Photoresist for Direct Photolithography Patterning, *Adv. Optical Mater.*, 2024, **12**, 2401106.
31 Y. Wang, I. Fedin, H. Zhang and D. V. Talapin, Direct Optical Lithography of Functional Inorganic Nanomaterials, *Science*, 2017, **357**, 385–388.
32 S. Lu, Z. Fu, F. Li, K. Weng, L. Zhou, L. Zhang, Y. Yang, H. Qiu, D. Liu, W. Qing, H. Ding, X. Sheng, M. Chen, X. Tang, L. Duan, W. Liu, L. Wu, Y. Yang, H. Zhang and J. Li, Beyond a Linker: The Role of Photochemistry of Crosslinkers in the Direct Optical Patterning of Colloidal Nanocrystals, *Angew. Chem., Int. Ed.*, 2022, **61**, e202202633.
33 J. Yang, M. Lee, S. Y. Park, M. Park, J. Kim, N. Sitapure, D. Hahm, S. Rhee, D. Lee, H. Jo, Y. H. Jo, J. Lim, J. Kim, T. J. Shin, D. C. Lee, K. Kwak, J. S. Kwon, B. Kim, W. K. Bae and M. S. Kang, Nondestructive

Photopatterning of Heavy-Metal-Free Quantum Dots, *Adv. Mater.*, 2022, **34**, 2205504.

34 D. Hahm, J. Lim, H. Kim, J.-W. Shin, S. Hwang, S. Rhee, J. H. Chang, J. Yang, C. H. Lim, H. Jo, B. Choi, N. S. Cho, Y.-S. Park, D. C. Lee, E. Hwang, S. Chung, C.-m. Kang, M. S. Kang and W. K. Bae, Direct Patterning of Colloidal Quantum Dots with Adaptable Dual-Ligand Surface, *Nat. Nanotechnol.*, 2022, **17**, 952–958.

35 D. Liu, K. Weng, S. Lu, F. Li, H. Abudukeremu, L. Zhang, Y. Yang, J. Hou, H. Qiu, Z. Fu, X. Luo, L. Duan, Y. Zhang, H. Zhang and J. Li, Direct Optical Patterning of Perovskite Nanocrystals with Ligand Cross-Linkers, *Sci. Adv.*, 2022, **8**, eabm8433.

36 Z. Fu, S. F. Musolino, W. Qing, H. Li, F. J. de Zwart, Z. Zheng, M. Cai, Y. Gao, B. de Bruin, X. Dai, J. E. Wulff and H. Zhang, Direct Photopatterning of Colloidal Quantum Dots with Electronically Optimized Diazirine Cross-Linkers, *J. Am. Chem. Soc.*, 2024, **146**, 28895–28905.

37 D. Liu, K. Weng, H. Zhao, S. Wang, H. Qiu, X. Luo, S. Lu, L. Duan, S. Bai, H. Zhang and J. Li, Nondestructive Direct Optical Patterning of Perovskite Nanocrystals with Carbene-Based Ligand Cross-Linkers, *ACS Nano*, 2024, **18**, 6896–6907.

38 J. Guan, J. Ma, L. Zhou, Y. Zou, L. Ye, W. Hou, P.-k. Zhang, X. Dai, H. Zhang, D. V. Talapin and Y. Wang, Direct Ambient Photopatterning of RGB Quantum Dots for Light-Emitting Diodes with EQE Exceeding 20, *Nat. Commun.*, 2025, **16**, 9689.

39 Z. Fu, L. Zhou, Y. Yin, K. Weng, F. Li, S. Lu, D. Liu, W. Liu, L. Wu, Y. Yang, H. Li, L. Duan, H. Xiao, H. Zhang and J. Li, Direct Photo-Patterning of Efficient and Stable Quantum Dot Light-Emitting Diodes *via* Light-Triggered, Carbocation-Enabled Ligand Stripping, *Nano Lett.*, 2023, **23**, 2000–2008.

40 Q. Nie, J. Fan, R. Xu, Z. Yao, Y. Xiao, C. Xiang, L. Qian and T. Zhang, Direct Optical Patterning of Quantum Dot Light-Emitting Diodes Based on Ultrafast, Low-Energy, Site Controlled Click Chemistry Reaction, *Adv. Funct. Mater.*, 2025, **35**, 2420829.

41 J.-A. Pan, H. Cho, I. Coropceanu, H. Wu and D. V. Talapin, Stimuli-Responsive Surface Ligands for Direct Lithography of Functional Inorganic Nanomaterials, *Acc. Chem. Res.*, 2023, **56**, 2286–2297.

42 S. Y. Park, S. Lee, J. Yang and M. S. Kang, Patterning Quantum Dots *via* Photolithography: A Review, *Adv. Mater.*, 2023, **35**, 2300546.

43 S. Baek and J. S. Son, Recent Advances in Direct Optical Patterning of Inorganic Materials and Devices, *Adv. Phys. Res.*, 2024, **3**, 2300069.

44 Y. Yang, J. Guan, N. Zhang, L. Ru, Y. Zou and Y. Wang, Advances in Direct Optical Lithography of Nanomaterials, *J. Mater. Chem. A*, 2024, **12**, 32505–32525.

45 Y. Qiu, Y. Yu, S. Wang and M. Chen, Advances in Quantum Dot Direct Photolithographic Patterning, *ACS Mater. Lett.*, 2024, **6**, 3176–3189.

46 M. Ibáñez, S. C. Boehme, R. Buonsanti, J. De Roo, D. J. Milliron, S. Ithurria, A. L. Rogach, A. Cabot, M. Yarema, B. M. Cossairt, P. Reiss, D. V. Talapin, L. Protesescu, Z. Hens, I. Infante, M. I. Bodnarchuk, X. Ye, Y. Wang, H. Zhang, E. Lhuillier, V. I. Klimov, H. Utzat, G. Rainò, C. R. Kagan, M. Cargnello, J. S. Son and M. V. Kovalenko, Prospects of Nanoscience with Nanocrystals: 2025 Edition, *ACS Nano*, 2025, **9**, 1012–1057.

47 S. Maeng and H. Cho, Direct Optical Lithography: Toward Nondestructive Patterning of Nanocrystal Emitters, *Acc. Mater. Res.*, 2025, **6**, 393.

48 N. Lee, D. A. Taylor, D. Choi, D. Kwak and J.-S. Lee, Advances in Photopatterning of Quantum Dots: Mechanisms, Materials, and Device Applications, *ACS Energy Lett.*, 2026, **11**, 1495–1513.

49 Y. Wang, J.-A. Pan, H. Wu and D. V. Talapin, Direct Wavelength-Selective Optical and Electron-Beam Lithography of Functional Inorganic Nanomaterials, *ACS Nano*, 2019, **13**, 13917–13931.

50 H. Cho, J. A. Pan, H. Wu, X. Lan, I. Coropceanu, Y. Wang, W. Cho, E. A. Hill, J. S. Anderson and D. V. Talapin, Direct Optical Patterning of Quantum Dot Light-Emitting Diodes *via in Situ* Ligand Exchange, *Adv. Mater.*, 2020, **32**, 2003805.

51 L. Li, S. Chakrabarty, K. Spyrou, C. K. Ober and E. P. Giannelis, Studying the Mechanism of Hybrid Nanoparticle Photoresists: Effect of Particle Size on Photopatterning, *Chem. Mater.*, 2015, **27**, 5027–5031.

52 M. H. V. Werts, M. Lambert, J.-P. Bourgoin and M. Brust, Nanometer Scale Patterning of Langmuir−Blodgett Films of Gold Nanoparticles by Electron Beam Lithography, *Nano Lett.*, 2002, **2**, 43–47.

53 F. Palazon, M. Prato and L. Manna, Writing on Nanocrystals: Patterning Colloidal Inorganic Nanocrystal Films through Irradiation-Induced Chemical Transformations of Surface Ligands, *J. Am. Chem. Soc.*, 2017, **139**, 13250–13259.

54 D. B. Dement, M. K. Quan and V. E. Ferry, Nanoscale Patterning of Colloidal Nanocrystal Films for Nanophotonic Applications Using Direct Write Electron Beam Lithography, *ACS Appl. Mater. Interfaces*, 2019, **11**, 14970–14979.

55 J. Yang, D. Hahm, K. Kim, S. Rhee, M. Lee, S. Kim, J. H. Chang, H. W. Park, J. Lim, M. Lee, H. Kim, J. Bang, H. Ahn, J. H. Cho, J. Kwak, B. Kim, C. Lee, W. K. Bae and M. S. Kang, High-Resolution Patterning of Colloidal Quantum Dots *via* Non-Destructive, Light-Driven Ligand Crosslinking, *Nat. Commun.*, 2020, **11**, 2874.

56 S. Maeng, S. J. Park, J. Lee, H. Lee, J. Choi, J. K. Kang and H. Cho, Direct Photocatalytic Patterning of Colloidal Emissive Nanomaterials, *Sci. Adv.*, 2023, **9**, eadi6950.

57 W. Qing, Y. Si, M. Cai, L. Zhou, L. Wu, Z. Hou, D. Liu, X. Tian, W. Liu, L. Lin and H. Zhang, Photosensitizer-Assisted Direct 2D Patterning and 3D Printing of Colloidal Quantum Dots, *Nano Res.*, 2024, **17**, 10460–10466.

58 J.-A. Pan, Z. Rong, Y. Wang, H. Cho, I. Coropceanu, H. Wu and D. V. Talapin, Direct Optical Lithography of Colloidal Metal Oxide Nanomaterials for Diffractive Optical

Elements with 2π Phase Control, *J. Am. Chem. Soc.*, 2021, **143**, 2372–2383.
59 J. Ko, J. H. Chang, B. G. Jeong, H. J. Kim, J. F. Joung, S. Park, D. H. Choi, W. K. Bae and J. Bang, Direct Photolithographic Patterning of Colloidal Quantum Dots Enabled by UV Crosslinkable and Hole-Transporting Polymer Ligands, *ACS Appl. Mater. Interfaces*, 2020, **12**, 42153–42160.
60 J. Ko, K. Ma, J. F. Joung, S. Park and J. Bang, Ligand-Assisted Direct Photolithography of Perovskite Nanocrystals Encapsulated with Multifunctional Polymer Ligands for Stable, Full-Colored, High-Resolution Displays, *Nano Lett.*, 2021, **21**, 2288–2295.
61 P. Xiao, J. Ma, Z. Zhang, Y. Zou, H. Luo, J. Guan, J. Zhang, L. Zhou, W. Hou, P. Zhang, D. V. Talapin and Y. Wang, Ligand-Engineered Direct Optical Lithography of Nanocrystals with Industrially Compatible Solvents, *ACS Nano*, 2025, **19**, 14509–14520.
62 S. Shin, K. Kang, H. Jang, N. Gwak, S. Kim, T. A. Kim and N. Oh, Ligand-Crosslinking Strategy for Efficient Quantum Dot Light-Emitting Diodes *via* Thiol-Ene Click Chemistry, *Small Methods*, 2023, **7**, 2300206.
63 N. Lee, D. Choi, K.-J. Ko, H.-S. Kim, J. Yu and J.-S. Lee, Direct Optical Lithography Using Diazirine Cross-Linker for Quantum Dot Light Emitting Diodes and Enhancing Photoluminescence Quantum Yield through Post-Treatment, *ACS Nano*, 2025, **19**, 22253–22261.
64 H. Seo, S. Z. Hassan, Y. J. Kim, T. Lee, G. W. Baek, C. So, D. S. Chung and J. Kwak, Direct Photolithography of Colloidal Inp-Based Quantum Dots Utilizing the Photoligation Method, *Chem. Mater.*, 2025, **37**, 1424–1431.
65 J.-M. Kim, D. Choi, N. Lee, W.-S. Chae, H.-S. Kim, J. Yu and J.-S. Lee, Role of Conjugated Structure of Cross-linkers in Patterned QLEDs, *Nano Lett.*, 2025, **25**, 10435–10441.
66 S. Maeng, J. Kim, T. Kim, S. Lee, S. Han, S. Park, C. Kim, J. Kim, J.-Y. Lee and H. Cho, Dual-Strategy Direct Photocatalytic Patterning for Efficient Perovskite Nanocrystal LED Displays, *Adv. Mater.*, 2025, **37**, e08217.
67 Y. Lee, J. Shin, S. Shin, E. A. Kim, J. Y. Lee, N. Gwak, S. Kim, J. Seo, H. Kong, D. Yeo, J. Na, S. Kim, J. Lee, S.-Y. Cho, J. Lee, T. A. Kim and N. Oh, *Adv. Mater.*, 2025, **37**, 2415436.
68 J.-A. Pan, H. Wu, A. Gomez, J. C. Ondry, J. Portner, W. Cho, A. Hinkle, D. Wang and D. V. Talapin, Ligand-Free Direct Optical Lithography of Bare Colloidal Nanocrystals *Via* Photo-Oxidation of Surface Ions with Porosity Control, *ACS Nano*, 2022, **16**, 16067–16076.
69 H. Baek, S. Kang, J. Heo, S. Choi, R. Kim, K. Kim, N. Ahn, Y.-G. Yoon, T. Lee, J. B. Chang, K. S. Lee, Y.-G. Park and J. Park, Insights into Structural Defect Formation in Individual InP/ZnSe/ZnS Quantum Dots under Uv Oxidation, *Nat. Commun.*, 2024, **15**, 1671.
70 Z. Chen, Z. Man, S. Rao, J. Zhao, S. Wang, R. Zhang, F. Teng and A. Tang, Rigid Crosslinker-Assisted Nondestructive Direct Photolithograph for Patterned QLED Displays, *Light Sci. Appl.*, 2025, **14**, 251.
71 K. A. Schnapp, R. Poe, E. Leyva, N. Soundararajan and M. S. Platz, Exploratory Photochemistry of Fluorinated Aryl Azides. Implications for The Design of Photoaffinity Labeling Reagents, *Bioconjug. Chem.*, 1993, **4**, 172–177.
72 W. T. Borden, N. P. Gritsan, C. M. Hadad, W. L. Karney, C. R. Kemnitz and M. S. Platz, The Interplay of Theory and Experiment in The Study of Phenylnitrene, *Acc. Chem. Res.*, 2000, **33**, 765–771.
73 N. P. Gritsan, A. D. Gudmundsdóttir, D. Tigelaar, Z. Zhu, W. L. Karney, C. M. Hadad and M. S. Platz, A Laser Flash Photolysis and Quantum Chemical Study of The Fluorinated Derivatives of Singlet Phenylnitrene, *J. Am. Chem. Soc.*, 2001, **123**, 1951–1962.
74 D. E. Westmoreland, R. López-Arteaga and E. A. Weiss, N-Heterocyclic Carbenes as Reversible Exciton-Delocalizing Ligands for Photoluminescent Quantum Dots, *J. Am. Chem. Soc.*, 2020, **142**, 2690–2696.
75 L. Du, N. A. Nosratabad, Z. Jin, C. Zhang, S. Wang, B. Chen and H. Mattoussi, Luminescent Quantum Dots Stabilized by N-Heterocyclic Carbene Polymer Ligands, *J. Am. Chem. Soc.*, 2021, **143**, 1873–1884.
76 Z. Zhai, C. Gu, W. Wang, H. Tan, C. Han, T. Zhang and C. Xiang, Nondestructive Direct Photolithography of Colloidal Quantum Dots Enabled by Benzophenone-Based Crosslinkers, *Nano Res.*, 2025, **18**, 94907980.
77 J. Ren, B. Dong, Y. Liao, L. Liu, C. Zhang, X. Zhou, H. Liu, F. Liu, L. Chen and Y. Wang, Highly Luminescent Photo-Crosslinkable Perovskite Nanocrystals: Advancing Direct Optical Patterning, 3D Painting, and Backlight Displays, *Adv. Funct. Mater.*, 2026, e29700.
78 Y. Huo, C. Luo, C. Wu, Z. Ren, H. Wang, D. Zhu, L. Wang, X. Zhou, Z. Zheng, X. Wang and Y. Chen, Ambient Direct Lithography Patterning of Ultra-Stable Perovskite Quantum Dots for High-Resolution Light-Emitting Diodes, *Adv. Funct. Mater.*, 2025, **35**, 2504261.
79 M. D. Tessier, D. Dupont, K. De Nolf, J. De Roo and Z. Hens, Economic and Size-Tunable Synthesis of InP/ZnE (E = S, Se) Colloidal Quantum Dots, *Chem. Mater.*, 2015, **27**, 4893–4898.
80 J. L. Stein, W. M. Holden, A. Venkatesh, M. E. Mundy, A. J. Rossini, G. T. Seidler and B. M. Cossairt, Probing Surface Defects of Inp Quantum Dots Using Phosphorus Kα and Kβ X-Ray Emission Spectroscopy, *Chem. Mater.*, 2018, **30**, 6377–6388.
81 J. Shamsi, A. S. Urban, M. Imran, L. De Trizio and L. Manna, Metal Halide Perovskite Nanocrystals: Synthesis, Post-Synthesis Modifications, and Their Optical Properties, *Chem. Rev.*, 2019, **119**, 3296–3348.
82 Y. Jiang, C. Sun, J. Xu, S. Li, M. Cui, X. Fu, Y. Liu, Y. Liu, H. Wan, K. Wei, T. Zhou, W. Zhang, Y. Yang, J. Yang, C. Qin, S. Gao, J. Pan, Y. Liu, S. Hoogland, E. H. Sargent, J. Chen and M. Yuan, Synthesis-on-Substrate of Quantum Dot Solids, *Nature*, 2022, **612**, 679–684.
83 A. Fakharuddin, M. K. Gangishetty, M. Abdi-Jalebi, S.-H. Chin, A. R. Yusoff, D. N. Congreve, W. Tress, F. Deschler, M. Vasilopoulou and H. J. Bolink, Perovskite Light-Emitting Diodes, *Nat. Electron.*, 2022, **5**, 203–216.
84 S. Lim, S. Han, D. Kim, J. Min, J. Choi and T. Park, Key Factors Affecting the Stability of $CsPbI_3$ Perovskite

Quantum Dot Solar Cells: A Comprehensive Review, *Adv. Mater.*, 2023, **35**, e2203430.
85 D. Kim, T. Yun, S. An and C. L. Lee, How to Improve the Structural Stabilities of Halide Perovskite Quantum Dots: Review of Various Strategies to Enhance the Structural Stabilities of Halide Perovskite Quantum Dots, *Nano Converg.*, 2024, **11**, 4.
86 W. Y. E. Ong, Y. Z. D. Tan, L. J. Lim, T. G. Hoang and Z.-K. Tan, Crosslinkable Ligands for High-Density Photo-Patterning of Perovskite Nanocrystals, *Adv. Mater.*, 2024, **37**, 2409564.
87 H. Furukawa, K. E. Cordova, M. O'Keeffe and O. M. Yaghi, The Chemistry and Applications of Metal-Organic Frameworks, *Science*, 2013, **341**, 1230444.
88 A. Bétard and R. A. Fischer, Metal-Organic Framework Thin Films: From Fundamentals to Applications, *Chem. Rev.*, 2012, **112**, 1055–1083.
89 M. D. Allendorf, R. Dong, X. Feng, S. Kaskel, D. Matoga and V. Stavila, Electronic Devices Using Open Framework Materials, *Chem. Rev.*, 2020, **120**, 8581–8640.
90 I. Stassen, N. Burtch, A. Talin, P. Falcaro, M. Allendorf and R. Ameloot, An Updated Roadmap for The Integration of Metal-Organic Frameworks with Electronic Devices and Chemical Sensors, *Chem. Soc. Rev.*, 2017, **46**, 3185–3241.
91 X. Tian, F. Li, Z. Tang, S. Wang, K. Weng, D. Liu, S. Lu, W. Liu, Z. Fu, W. Li, H. Qiu, M. Tu, H. Zhang and J. Li, Crosslinking-Induced Patterning of Mofs by Direct Photo- and Electron-Beam Lithography, *Nat. Commun.*, 2024, **15**, 2920.
92 Z. Zhu, F. Li, J. Li, Q. Chen, W. Li, Z. Tang, W. Xu, W. Shen, T. H. Tao, L. Sun, Y. Fu and M. Tu, Direct Optical Patterning of Metal–Organic Frameworks *via* Photoacid–Induced Etching, *ACS Nano*, 2024, **18**, 19628–19635.
93 X. Tian, W. Li, F. Li, M. Cai, Y. Si, H. Tang, H. Li and H. Zhang, Direct Photopatterning of Zeolitic Imidazolate Frameworks *via* Photoinduced Fluorination, *Angew. Chem., Int. Ed.*, 2025, **64**, 202500476.
94 S. V. Murphy and A. Atala, 3D Bioprinting of Tissues and Organs, *Nat. Biotechnol.*, 2014, **32**, 773–785.
95 J. M. Pearce, Building Research Equipment with Free, Open-Source Hardware, *Science*, 2012, **337**, 1303–1304.
96 K. Sun, T.-S. Wei, B. Y. Ahn, J. Y. Seo, S. J. Dillon and J. A. Lewis, 3D Printing of Interdigitated Li-Ion Microbattery Architectures, *Adv. Mater.*, 2013, **25**, 4539–4543.
97 A. T. Polonsky and T. M. Pollock, Closing The Science Gap in 3D Metal Printing, *Science*, 2020, **368**, 583–584.
98 E. MacDonald and R. Wicker, Multiprocess 3D Printing for Increasing Component Functionality, *Science*, 2016, **353**, aaf2093.
99 S. Liu, Z. Hou, L. Lin, F. Li, Y. Zhao, X. Li, H. Zhang, H. Fang, Z. Li and H. Sun, 3D Nanoprinting of Semiconductor Quantum Dots by Photoexcitation-Induced Chemical Bonding, *Science*, 2022, **377**, 1112–1116.
100 F. Li, S. Liu, W. Liu, Z. Hou, J. Jiang, Z. Fu, S. Wang, Y. Si, S. Lu, H. Zhou, D. Liu, X. Tian, H. Qiu, Y. Yang, Z. Li, X. Li, L. Lin, H. Sun, H. Zhang and J. Li, 3D Printing of Inorganic Nanomaterials by Photochemically Bonding Colloidal Nanocrystals, *Science*, 2023, **381**, 1468–1474.
101 C. Mao, S. Ju, J. Zheng, Y. Zheng, Z. Xu, L. Lin, H. Hu, K. Yang, T. Guo and F. Li, Ultra-High-Resolution Perovskite Quantum Dot Light-Emitting Diodes, *Adv. Optical Mater.*, 2023, **11**, 2202058.
102 C. Luo, Z. Zheng, Y. Ding, Z. Ren, H. Shi, H. Ji, X. Zhou and Y. Chen, High-Resolution, Highly Transparent, and Efficient Quantum Dot Light-Emitting Diodes, *Adv. Mater.*, 2023, **35**, 2303329.
103 H. Li, J. Zhang, W. Wen, Y. Zhao, H. Gao, B. J, Y. Wang, L. Jiang and Y. Wu, Highly Efficient Light-Emitting Diodes *via* Self-Assembled InP Quantum Dots, *Nat. Commun.*, 2025, **16**, 4257.
104 Y. Lian, Y. Wang, Y. Yuan, Z. Ren, W. Tang, Z. Liu, S. Xing, K. Ji, B. Yuan, Y. Yang, Y. Gao, S. Zhang, K. Zhou, G. Zhang, S. D. Stranks, B. Zhao and D. Di, Downscaling Micro- and Nano-Perovskite LEDs, *Nature*, 2025, **640**, 62–68.
105 D. Hahm, J. Park, I. Jeong, S. Rhee, T. Lee, C. Lee, S. Chung, W. K. Bae and S. Lee, Surface Engineered Colloidal Quantum Dots for Complete Green Process, *ACS Appl. Mater. Interfaces*, 2020, **12**, 10563–10570.
106 Z. Fu, Z. Zheng, Y. Xie, H. Abudukeremu, L. Zhou, S. Zang, K. Tian, Q. Liu, Y. Li and H. Zhang, Direct Photopatterning and Erasing of Quantum Dots *via* Ligand Photoisomerization, *Chem. Commun.*, 2026, **62**, 4089–4093.